VEGETATION CLASSIFICATION AND SURVEY

International Association for Vegetation Science (IAVS)

Vegetation Classification and Survey 6: 279–299
doi: 10.3897/VCS.157787

RESEARCH PAPER SPECIAL COLLECTION ISLANDS AND ARCHIPELAGOS

Characterizing and mapping coastal vegetation on a sea island in the southeastern USA

Cody Goodson[1], John Holloway[2], Zak H. Bartholomew[1], Anne C. Axel[1], Pamela Puppo[1], Peyton Debowsky[1], Kyle A. Palmquist[1]

1 *Department of Biological Sciences, Marshall University, Huntington, West Virginia, USA*

2 *Environmental Division – Natural Resources Section, The Marine Corps Recruit Depot Parris Island, Parris Island, South Carolina, USA*

Corresponding author: Kyle A. Palmquist (palmquist@marshall.edu)

Academic editor: Jorge Capelo
Received 12 May 2025 ♦ **Accepted** 25 October 2025 ♦ **Published** 23 December 2025

Abstract

Questions: Our objectives were to classify and map coastal vegetation types on a sea island that is undergoing rapid change from storm surge intensification and sea-level rise (SLR). **Study area:** The Marine Corps Recruit Depot Parris Island (MCRDPI) is a sea island in South Carolina, USA, dominated by tidal salt marshes with large, inland forested areas and developed areas supporting Marine Corps training activities. The climate is humid subtropical. **Methods:** We established 57 permanent vegetation plots within all the major coastal vegetation types present on the island, made detailed plant community measurements, and characterized the main environmental variables associated with each vegetation type. We employed cluster analysis and non-metric multidimensional scaling ordination to delineate these types based on vegetation plot data and then cross-walked those types onto existing associations within the United States National Vegetation Classification (USNVC). Finally, supervised deep learning classification was employed on 0.5 m high-resolution RBG imagery to map the distribution of vegetation types and other land cover types. **Results:** We identified four marsh associations and eight forest/woodland associations. The distributions of these vegetation types were primarily related to salinity and elevation. In addition to these 12 vegetation types, we mapped 11 additional land cover types for a total of 23 distinct classes. The marsh types dominated the landscape, covering ~57% of the classified area, while forest types covered ~13%. Accuracy assessment yielded an overall accuracy of 62% and a Kappa statistic of 0.6. **Conclusions:** We identified 11 existing USNVC vegetation types that are widely distributed in the southeastern USA and mapped their spatial distribution. The permanent vegetation plots and vegetation map provide fundamental baseline information that can be used to monitor the effects of climate change on coastal vegetation, evaluate wildlife habitat use by species of conservation concern, and facilitate decision-making in a region that has been identified as a global hotspot of salt marsh loss.

Taxonomic reference: Weakley (2022).

Syntaxonomic reference: USNVC (2025).

Abbreviations: DBH = diameter at breast height; MCRDPI = Marine Corps Recruit Depot Parris Island; ROI = Regions of Interest; SLR = Sea-level rise; TEC = total exchange capacity; USNVC = United States National Vegetation Classification.

Keywords

Climate change, coastal vegetation, deep learning, sea-level rise, supervised classification, vegetation classification, vegetation mapping

PENSOFT

Copyright: This is an open access article distributed under the terms of the CC0 Public Domain Dedication.

Introduction

Coastal ecosystems are among the most functionally important habitats and are among the most sensitive to climate change. Upland forests and wetlands along the coast significantly buffer storm surges and the longer-term effects of erosion (Watson and Byrne 2009; Sousa et al. 2010; Feagin et al. 2010; Alizad et al. 2018; White et al. 2022). Coastal wetlands (i.e., salt marshes) have significant filtration capabilities that can assimilate pollutants and prevent eutrophication and sequester large amounts of carbon above- and belowground, thus acting as carbon sinks (Sousa et al. 2010; Humphreys et al. 2021; White et al. 2022). Coastal landscapes also support a diverse array of wildlife that rely on these habitats including migratory birds, reptiles, amphibians, rodents, and invertebrate species (Simas et al. 2001; Rosencranz et al. 2019; Marcot et al. 2020; Anderson et al. 2022; White et al. 2022).

Native coastal vegetation is well adapted to the cyclic rise and fall of the tides. These plants trap sediment, mediating accretion of salt marsh substrates and potentially succession to mature, coastal forests. However, climate change is amplifying the intensity and frequency of disturbance, and rapidly altering conditions to which the dominant species are adapted (Feagin et al. 2010; Naumann et al. 2009; Kearney et al. 2019). Eustatic sea-level rise (SLR) resulting from rising ocean temperatures and melting land ice (Simas et al. 2001; He and Silliman 2019) is imposing significant stress on coastal vegetation (Warren and Niering 1993; Lucas and Carter 2013; Alizad et al. 2018; Cahoon et al. 2021) and the intensity of storm surge events associated with tropical storms are increasing (Donnelly et al. 2001; Webster et al. 2005; He and Silliman 2019; White et al. 2022). Coastal habitats can respond in very different ways to these disturbances. Some marshes experience submergence and conversion to open water (Reed 1995; Simas et al. 2001), while other areas accrete sediment and keep pace with SLR (Field et al. 2016; Kirwan and Gedan 2019; Rosencranz et al. 2019). If saltwater intrusion begins to compromise upland forest habitats, then marshes may migrate upland, driving habitat conversion (Murray et al. 2022; White et al. 2022). These differential responses are modulated by site-specific conditions, so a critical need is to characterize the composition and spatial distribution of coastal ecosystems in relation to environmental variables to improve our understanding of the impacts SLR may have on coastal habitats (Raposa et al. 2017). Accurate mapping of vegetation types is vital for tracking shifts in species distributions and to understand how plant communities are responding to changing conditions.

Coastal vegetation is highly zonal, with high compositional turnover at small spatial scales. The most influential environmental variables affecting its distribution are salinity (Reed 1995; Watson and Byrne 2009; Cunha-Lignon et al. 2011; Du and Hesp 2020; Humphreys et al. 2021) and inundation (Warren and Niering 1993; Tiner 2013; Alizad et al. 2018). Coastal plant communities assemble along a salinity gradient which is influenced by hydroperiod, the amount of time a given area is inundated (Watson and Byrne 2009; Tiner 2013; Woods et al. 2020) and relatedly, elevation (Costa et al. 2003). Low marsh species are adapted to high frequency tidal dynamics and high salinity. Species assemblages further inland generally occur at higher elevations and thus experience less extreme inundation and salinity (Tiner 2013). However, topographic variation can drive the formation of distinct vegetation types. For example, salt flats are a high marsh vegetation type that form when seawater gets trapped in low-lying depressions as the tide recedes and the water evaporates leaving behind high concentrations of salt (USNVC 2025). Only halophytic species exist in these locations (Bertness et al. 1992; Tiner 2013). Otherwise, salinity continues to decline further inland as elevation increases and exposure to salt spray decreases, where eventually more diverse assemblages that are less salt-tolerant can form (i.e. oligohaline vegetation characterized by salinity of 0.5–5 parts per thousand) (Kirwan et al. 2007; White et al. 2022).

Vegetation classification and mapping is a useful approach for quantifying the spatial distribution of vegetation types and characterizing how vegetation composition varies along environmental gradients. Vegetation maps are useful for conservation planning, management, and other decision-making (Jennings et al. 2009). For example, they can be used to understand shifts in the distributions of vegetation types over time, prioritizing areas for management activities, and identifying suitable habitat for wildlife species of conservation concern (Peet et al. 2012). Utilizing a widely accepted, comprehensive vegetation classification can improve the comparability and replicability of findings. The United States National Vegetation Classification (USNVC) is a multi-level, hierarchical vegetation classification system that categorizes all existing natural and ruderal vegetation of the United States. Vegetation types are grouped at the highest level by physiognomy and at the finest level by floristics, while intermediate vegetation types incorporate information on climate, soil properties, biogeography, and natural dynamics (Franklin et al. 2012; Faber-Langendoen et al. 2014). The finest scale unit within the USNVC is the Association level, which describes specific occurrences of species assemblages, characterized by the presence of diagnostic species (USNVC 2025).

In this study, we integrated field-derived vegetation data from permanent vegetation plots and remote sensing to characterize coastal vegetation on the Marine Corps Recruit Depot Parris Island (MCRDPI), a sea island in South Carolina, USA. Our specific objectives were to: 1) Identify and describe the vegetation types present on MCRDPI; and 2) Create a vegetation map of MCRDPI. We crosswalked the vegetation types that were delineated from an analysis of plot data to USNVC Associations. We then mapped those Associations, along with other land cover types (e.g., water, infrastructure) to create a continuous land cover and vegetation map of MCRDPI, which is critical to support ongoing management of natural resources and wildlife species of conservation concern, such as the eastern diamondback rattlesnake (*Crotalus adamanteus*)

and the southern fox squirrel (*Sciurus niger niger*). In addition, this work provides fundamental baseline knowledge on the current distribution of vegetation types on MCRDPI to facilitate future efforts to characterize changes in vegetation in relation to SLR, increased storm surge, and other anthropogenic factors. Additionally, identifying and mapping vegetation on MCRDPI and cross-walking it to existing USNVC Associations contributes to the supporting body of literature on the range and composition of these vegetation types, many of which are widely distributed throughout the Atlantic Coastal Plain and Gulf Coastal Plain regions of the southeastern USA.

Study area

Vegetation surveys were conducted on MCRDPI in Beaufort County, South Carolina, USA from May to July of 2022 and in July 2023. MCRDPI is a 3,256 ha sea island located in the North American Coastal Plain at the junction of the Beaufort and Broad Rivers (Figure 1). This region has been identified as a global hotspot of coastal habitat change due to the high relative rate of SLR and frequency of storm activity (Cazenave and Cozannet 2014; Rutledge et al. 2021; White et al. 2022) and contains plant communities that are widely distributed along the southeastern Atlantic and Gulf Coasts of the USA.

The climate is humid subtropical, characterized by hot, humid summers, and mild winters. The 30-year normal mean annual temperature and precipitation for 1991–2020 were 19.6 °C and 1144 mm respectively (NOAA 2023). The dominant soil series on MCRDPI is the Bohicket series, which is a silty clay loam Entisol that forms in coastal marshes from deposited marine sediment and is highly saline (Soil Survey Staff 2019). The organic layer often has fibrous roots from decomposing grass stems, it experiences daily tidal flooding, and has low permeability (Vepraskas et al. 2000). The soil in the forests are primarily Ultisols and Spodosols. The three most abundant series include Seabrook, Seewee, and Williman, which are acidic loamy sand soils formed from marine and fluvial sediments with thick sand horizons and a water table depth that is near the surface for most of the year (Soil Survey Staff 2019).

The dominant vegetation types are tidal salt marshes dominated by smooth cordgrass (*Spartina alterniflora*), along with salt flats and brackish marshes dominated by glasswort (*Salicornia* spp.) and other salt-tolerant graminoids and shrubs (e.g., *Borrichia frutescens*, *Distichlis spicata*, *Juncus roemarianus*). In addition to salt and brackish marshes, large areas of MCRDPI are forested, including maritime forests that are near the ocean and are dominated by evergreen oaks (e.g., *Quercus virginiana*, *Q. hemisphaerica*), pine forests and woodlands dominated by slash pine (*Pinus elliottii*), and isolated patches of temperate deciduous forests. Other vegetation types include hummocks, saline shrublands, and salt scrub, which occur at transitions between high salt marsh and forests or on spits immediately adjacent to the open ocean. The developed infrastructure is primarily on the northern, upland portion of the island. This includes recruit housing, offices, and residential areas with small parcels of maintained fields and forests. Other major landmarks include a firing range, a public golf course, and an inactive airfield.

The MCRDPI Environmental Division conducts intermittent management (e.g., thinning and prescribed fire) primarily within the pine habitats to maintain open forest conditions for wildlife species of conservation concern that are open-habitat specialists, such as the eastern diamondback rattlesnake and southern fox squirrel, as well as to maintain recruit training areas. Salvage logging has also been implemented to remove woody debris after major storm damage, which last occurred after tropical storm Irma in 2017.

Methods

Site selection

In 2022 and 2023, 57 vegetation plots were established within the major vegetation types of MCRDPI, including representative vegetation from forest habitats (maritime forest, temperate deciduous forest, pine forest, and pine woodland) and marsh habitats (salt marsh, brackish marsh, salt flat, saline shrubland, and hummocks) (Figure 1). A few vegetation types were relatively rare and therefore not captured by our vegetation plots (i.e., salt scrub, dunes). Of the 27 forest sites, 21 were co-located with small mammal and herpetofauna survey sites (camera arrays) from a different study so that vegetation characteristics such as stand structure and herbaceous cover could be linked to occupancy for eastern diamondback rattlesnakes and small mammals, their primary food source.

To limit interference between the flora and fauna surveys, a set of five coordinates were randomly generated within a 10–50 m buffer zone of each array to identify the location of the vegetation plot. Each randomly generated point was then assessed based on a set of rejection criteria; the plot needed to be located within the same general vegetation type as the array (i.e., a forest plot should not extend out into the marsh), be at least 100 m from other vegetation survey plots, and be at least as far from roadsides as the fauna array. If these criteria were not met, the point was rejected, and the next coordinate was assessed. Additional forest sites ($N = 6$) were identified and surveyed in maritime forests ($N = 5$) and temperate deciduous forests ($N = 1$), which were under-represented by the 21 array sites. Finally, the remaining sites ($N = 30$) in the other major vegetation types (i.e., salt marsh, brackish marsh, salt flat, salt scrub, and hummock) were selected by generating random coordinate points in ArcGIS Pro within field-delineated marsh and hummock polygons (denoted with "MAR", Figure 1) since there was no existing vegetation map for MCRDPI. All coordinates generated were at least 100 m from each other. Sites were rejected if they were not safely accessible on foot or were within 10 m of a road.

Figure 1. Locations of the permanent vegetation plots. Plots labeled SMA1 – 21 were co-located with animal trapping arrays; SMA22 – 27 are forest plots added to capture forest types that were underrepresented by array sites (maritime forest, temperate deciduous forest). Plots labeled MAR were located in marsh habitats and hummocks, the latter representing vegetation intermediate between marsh and forest types.

Vegetation surveys

For each of the 57 sites, a vegetation plot was established using the selected random point as the origin, which served as one of the corners. For the forest sites, a 20 m × 20 m (400 m^2) plot was sampled. A 10 m × 10 m (100 m^2) plot was sampled for most of the other major vegetation types, hereafter referred to collectively as "marsh" sites. Smaller plots were used for the marsh sites due to the low diversity and high homogeneity of these habitats; larger plot sizes would not have added any new information and would have been more time-intensive. There were two hummocks that supported more species and warranted larger plot sizes to adequately capture species composition but were not large enough to permit the forest plot size (400 m^2). As a result, the plot sizes for those two hummocks were 200 m^2 and 300 m^2. For the marsh sites, each plot was oriented according to a randomly generated bearing; the forest sites were oriented on the same randomly generated bearing as the fauna arrays. Steel conduit that was 0.3 m in length was used to permanently mark the four plot corners to facilitate future re-sampling. For some of the marsh sites with deep silty soils, 0.9 m sections of rebar were used to mark two of the corners to facilitate relocation of the plots. A coordinate was taken at the origin of each plot using a BadElf Pro+ GPS unit (< 5 m accuracy).

At each site, a preliminary vegetation type (pine forest, pine woodland, maritime forest, temperate deciduous forest, low salt marsh, high salt marsh, brackish marsh, salt flat, salt scrub, hummock) was assigned in the field based on our a priori knowledge of existing vegetation types on MCRDPI. These field assignments helped us to later identify and interpret clusters and cross-walk them to USNVC Associations. All vascular plant species rooted within the plot were identified to the species level. Any plant individuals not identifiable to species in the field were collected, pressed, and later identified using Weakley (2022) and deposited in the Marshall University Herbarium. Total percentage cover for each species was estimated using the Carolina Vegetation Survey cover codes (1 = trace, 2 = 0–1%, 3 = 1–2%, 4 = 2–5%, 5 = 5–10%, 6 = 10–25%, 7 = 25–50%, 8 = 50–75%, 9 = 75–95%, 10 = >95%) to quantify species abundance (Peet et al. 1998).

Any signs of management (e.g., cut stumps, fire scars) and the general physiognomy of the habitat were noted. Finally, soil samples were taken from the top 30 cm of the soil in the center of each plot, dried for 48 to 72 hours at 40 °C, sieved through a 2 mm sieve, and then sent to Brookside Laboratories Inc. (New Bremen, OH) for analysis to determine soil texture, macro- and micro-nutrient availability, organic matter, pH, total exchange capacity (TEC), and base saturation. Salinity was measured in parts per thousand (ppt) using an Oakton EcoTestr™ CTS1 Pocket Conductivity, Salinity, and TDS Meter probe (Cole-Parmer, Vernon Hills, IL). The probe was immersed in 10 ml of each soil sample that had been mixed with 30 ml of distilled water for 30 seconds. Elevation was also derived for each site by intersecting site coordinates with the most recently available LiDAR- derived digital elevation model (1 m resolution) of MCRDPI from 2020 acquired from the Beaufort County, SC GIS office.

Vegetation type assignment

To delineate vegetation types on MCRDPI, we used cluster analysis and ordination, which were implemented in R version 4.2.0 (R Core Team 2022). First, we calculated a Bray-Curtis dissimilarity matrix from the abundance-weighted species composition data (plot, species, cover class code). Bray-Curtis dissimilarity is well suited for vegetation data, which are not generally normally distributed and contains many zeros (McCune and Grace 2002; Legendre and De Cáceres 2013). We then conducted a hierarchical agglomerative cluster analysis with flexible beta (β = –0.25; agnes function, cluster package in R, Maechler et al. 2022). Initially, we evaluated clustering solutions of clusters 2–20 (k = 2–20) to determine the optimal number of clusters indicated by the analysis. Optimality of the solutions was evaluated by calculating silhouette width (silhouette function, cluster package in R, Maechler et al. 2022) and interpreting plot level data including soil properties, physiognomy, habitat types assigned in the field, and species composition of each cluster. Silhouette width compares the average dissimilarity of a plot to that of each plot in its assigned cluster as well as to the average dissimilarity of the plots in the next closest (i.e., neighbor) cluster (Rousseeuw 1987). Species composition for each cluster was characterized using a constancy table, which displayed the percentage of plots within a cluster that each species was present in, as well as the average cover of that species within that cluster.

We employed fuzzy noise clustering as a final cluster validation assessment to address plots that did not seem to fit well with their assigned cluster (Dave 1991; De Cáceres et al. 2010). We passed our initial clustering solution into the new noise clustering framework (m = 1.1, δ = 0.7). The fuzzy clustering was collapsed into a hard clustering solution which was used to reevaluate the initial clustering solution. Other data were considered in this final evaluation, including our habitat types assigned to plots in the field, plot physiognomy, general vegetation descriptions, and the species constancy table.

After determining the optimal clustering solution (12 clusters), we then cross-walked each cluster onto an existing USNVC Association. To facilitate this task, we generated a new constancy table for the final clustering solution to identify the prevalent and diagnostic species within each cluster. We considered diagnostic species to be those that had 50% constancy or greater and occurred with an average cover of 2% or greater. In the results, we summarize the concept for each USNVC Association and demonstrate how our clusters are consistent with those Associations.

We then assessed the final clustering solution to help describe the vegetation types assigned to each cluster. We used non-metric multidimensional scaling (NMDS) ordination (metaMDS function, vegan package in R, Oksanen et al. 2022) to visualize the dissimilarities between sites and to identify which environmental variables were related to species compositional gradients. Dimensionality of the NMDS ordination was assessed by creating a stress plot for dimensions 1–10. Significant variables ($p < 0.05$) were overlaid as vectors onto the ordination (envfit function, vegan package in R, Oksanen et al. 2022). The variables included were percentage silt and sand, organic matter (%), calcium availability (mg/kg), total exchange capacity (meq/100 g), pH, salinity (ppt), and elevation (m). We also overlaid species richness to understand how it varied across plots and among the resulting clusters. The distributions of statistically significant environmental variables for plots within each vegetation type were also visualized using boxplots. The distributions of some variables were also plotted for just the forest vegetation types either because the variables were only relevant to these types (i.e., calcium availability and canopy cover), or to better visualize their distributions amongst these types (i.e., total exchange capacity and salinity).

Vegetation map

To create a vegetation map of MCRDPI, we obtained very high spatial resolution (0.5 m) RGB aerial imagery from 2022 from the Beaufort County GIS office. This imagery was collected by aircraft during the period of 1/11/2022 to 1/18/2022. We chose to use very high spatial resolution imagery due to the spatial complexity and compositional turnover of coastal vegetation over small spatial scales (Campbell et al. 2017). Prior to image classification, we performed top of atmosphere corrections.

Training data were collected both on the ground and from the RGB aerial imagery. In summer of 2022, in addition to training data associated with vegetation plots, we also recorded additional field training point coordinates in all existing vegetation types on MCRDPI, including some types for which we did not sample vegetation plots (i.e., dune, salt scrub, pine regeneration, successional shrubland, and yaupon forest). We augmented field-derived training points with user-defined Regions of

Interest (ROIs) selected from the imagery itself, based on our knowledge of vegetation type distributions in MCRDPI and image interpretation, an approach that has been widely implemented in other mapping studies (Campbell 2006; Schowengerdt 2007; Hladik et al. 2013). We used the imagery to collect training points for readily identifiable 'water' class and non-vegetated land cover types (i.e., buildings, pavement, and solar panels) that were ultimately collapsed into an 'infrastructure' class. Both field-derived and ROIs informed the extensive training sample collection required for deep learning (Maggiori et al. 2017; Ma et al. 2019), the classification algorithm we used to produce the vegetation map.

We implemented deep learning classification because of the high resolution and relatively small extent of the 2022 imagery. Traditional machine learning classification approaches such as Random Forest and Support Vector Machine (Osisanwo et al. 2017) can have issues classifying coarser scale vegetation types when spatial resolution is high because information on the spatial relationships between pixels is inherently lost during the processing of imagery by these approaches (Wang et al. 2021; Gonzalez-Perez et al. 2022). Trial runs with Random Forest resulted in a fragmented output in which plant individuals (mostly trees) were assigned to distinct vegetation types. Deep learning classification approaches are better at pattern recognition and perform well with the increased image complexity associated with high spatial resolutions (Ma et al. 2019; Tong et al. 2020; Gonzalez-Perez et al. 2022).

Deep learning was implemented in ArcGIS Pro using the deep learning image analyst tools on the 2022 raster clipped to the extent of MCRDPI. The training samples were exported as classified tile image chips (Export Training Data For Deep Learning Tool) and used to train a U-Net deep learning model with a resnet-34 backbone model (Train Deep Learning Model Tool). The output model was then used to conduct pixel-based supervised classification of the 2022 raster (Classify Pixels Using Deep Learning Tool). The resulting vegetation map contained 23 land cover types: pine forest with maritime influence, pine woodland with maritime influence, open pine woodland, pine regeneration, maritime forest, temperate deciduous forest, mixed forest, successional shrubland, yaupon forest, developed forest, soft marsh, hard marsh, brackish marsh, salt flat, salt scrub, saline shrubland, hummock, dune, beach, infrastructure, water, mowed lawn, and bare ground.

Misclassifications between classes with poor separability were manually corrected using the reclassifier tool in ARCGIS Pro to produce the final vegetation map. Manual reclassification was conducted for a few classes with poor separability due to a high degree of similarity between the spectral signatures and spatial characteristics of their pixels. The main class pairings with poor separability included brackish marsh and bare ground, developed forest and maritime forest, maritime forest and hummock, and open pine woodland and pine woodland with maritime influence. Additionally, mixed forest was difficult to distinguish from most other forested types because the canopy composition contained a mixture of tree species that dominate each of the other forest types, resulting in significant spectral overlap.

Accuracy assessment

An accuracy assessment was conducted to evaluate the performance of the supervised deep learning classification approach and to quantify the utility of the vegetation map as a management tool. Field surveys for the accuracy assessment were conducted in December 2023 and during June 3rd to July 30th, 2024. During December, 42 points were sampled with 483 additional points sampled during summer 2024 for a total of 525 validation points. Validation points were generated using a stratified random design for the 23 land cover types. To effectively balance estimation of user's accuracy (how often the class on the map will actually be present on the ground) and producer's accuracy (how often points on the ground were correctly assigned on the map) and maximize estimation of overall accuracy, we determined the sample size per land cover type based on proportional area but ensured that at least 15 validation points were sampled for each type by increasing the sample size of rare types above what proportional area would suggest (as recommended by Olofsson et al. 2014). The sample size for each type was calculated by multiplying its proportional area by the number of total anticipated survey points and ensuring that the minimum number of survey points was met (15 points per land cover type). Two land cover types, salt scrub and temperate deciduous forest, were so narrowly distributed that we were not able to sample the minimum of 15 points. In both cases, we sampled the maximum number of validation points for each type based on other validation point selection criteria (see below) ($N = 9$ for salt shrub and $N = 12$ for temperate deciduous forest).

Initially, 100 points were randomly generated for each land cover type. Additional points were generated for soft marsh and water to provide sufficient potential validation points given the large and mostly inaccessible areas they covered. Given the number and spread of potential validation points across MCRDPI, we chose a methodology for selecting validation points to survey that balanced a random design with the need to be efficient in surveying. The method involved working sequentially from one habitat type to another while also sampling other points in that same area. In some cases, we surveyed validation points of the same land cover type in close proximity and ensured there was a minimum distance of 50 m between those validation points. There was no minimum distance between validation points of different habitat types. When the next random point to survey was near a group of previously sampled points, we chose to reject it and moved to the next point. Towards the latter half of the field season, the point selection protocol was altered to emphasize validation points for land cover types with larger sampling needs (i.e., soft marsh, water).

In the field, a Bad Elf Pro+ GPS was used to navigate to the coordinate of each validation point. At each point, we

set up a 5 m radius circle plot and recorded the GPS position at plot center. A Survey123 form was used to collect data for each plot. We recorded a coarse land cover type (wetland, forest, water, non-vegetated, anthropogenic), one of the 23 fine land cover types described above, physiognomy (forest, woodland, shrubland, herbaceous, non-vegetated), and estimates of cover for dominant species by strata (tree, shrub, herbaceous). This data informed which land cover type the validation point was assigned to in the field. For example, certain land cover types like pine forest with maritime influence and open pine woodland were defined by dominant tree species and percent of tree canopy cover.

During field surveys, we attempted to place the plot center as close as possible to the validation point's coordinates. However, under the best conditions, the estimated accuracy of the Bad Elf receiver was around 2 m, with an average estimated accuracy of 3 m. This meant that when recording the plot center, there was the potential for the recorded point to be off from the validation point location. To ensure that we were comparing the recorded GPS survey point with what was represented on the map, we extracted the land cover type from the vegetation map at that recorded GPS coordinate.

To determine the accuracy of the vegetation map, we generated a confusion matrix, which compared the vegetation classification map's expected land cover type to the land cover type recorded in the field. We also calculated user's accuracy, producer's accuracy, the overall accuracy of the map, and the kappa coefficient. All calculations were performed with RStudio 04.2 Build 764 (RStudio Team 2024) using R version 4.2.2 (R Core Team 2022).

Results

Vegetation types

During the vegetation surveys, a total of 198 vascular plant species were identified. Visualization of plot level dissimilarity revealed three distinct groups of vegetation plots in the dendrogram (Figure 2). The blue branch contains all the hard and soft marsh sites, which were monotypic stands of smooth cordgrass (*Spartina alterniflora*). The red branch includes high marsh vegetation types such as salt flats, saline shrublands, and brackish marshes that have some compositional overlap of halophytic species. The gray branch includes all forest sites, which were much more diverse and heterogeneous as indicated by the complex branching within the dendrogram (Figure 2).

The hierarchical agglomerative clustering results in conjunction with silhouette width yielded an initial 11-cluster solution. After assessing this initial solution using various cluster validity techniques, some plots were moved to their nearest neighbor clusters or to new clusters. Specifically, one site that was clustered by itself was merged with another existing cluster, seven sites were moved to their nearest neighbor cluster, and two sites were moved to other clusters. Afterwards, a final 12-cluster solution was selected as the optimal clustering of vegetation plots (Table 1, Suppl. material 3). After reviewing soil and environmental data and the species constancy tables, a USNVC Association was assigned to each of the 12 clusters. Of these Associations, four belong to the Salt Marsh Formation and 8 belong to the Warm Temperate Forest and Woodland Formation (Table 1).

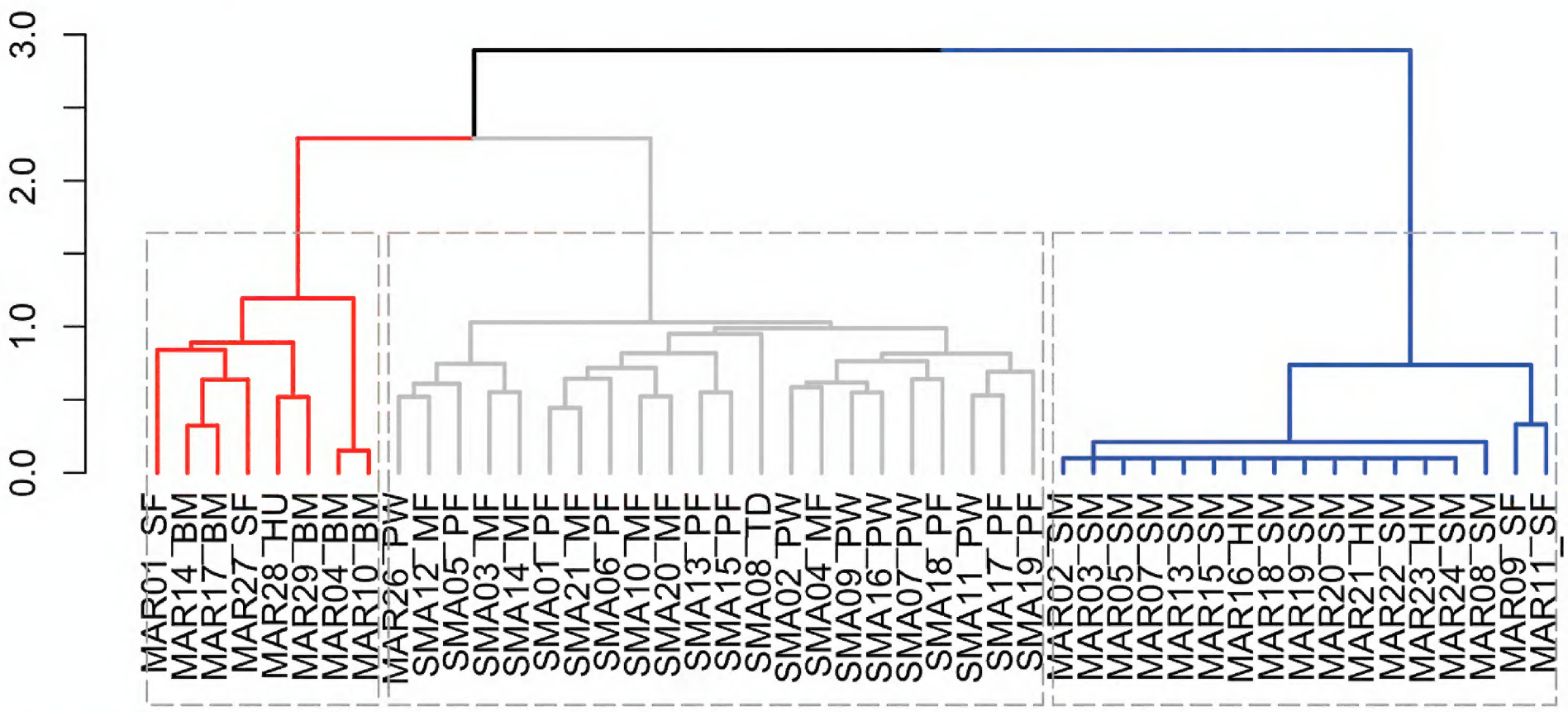

Figure 2. Dendrogram of vegetation plots. Most of the plots labeled "SMA" were co-located with animal trapping arrays; SMA22 – SMA27 were additional forest plots added to capture types that were underrepresented by array sites (*N* = 6). Plots labeled "MAR" represent low and high marsh vegetation types as well as hummocks, which are intermediate between forest and marsh types. The subsequent two letter codes represent a priori habitat types assigned to each plot: PF (pine forest), PW (pine woodland), maritime forest (WF), temperate deciduous forest (TD), hummock (HU), salt flat (SF), saline shrubland (SS), brackish marsh (BM), soft marsh (SM), and hard marsh (HM). Dashed, gray boxes indicate plots belonging the three-cluster solution. Red branches represent high marsh types, gray branches represent forest types, and blue branches represent low marsh types.

Table 1. USNVC Associations assigned to each of the 12 final clusters that emerged from quantitative analysis of vegetation plot data. Shown is a coarse vegetation type (marsh, hummock, or forest), the number of plots in each cluster, the cluster number, and the USNVC Association listed as the unique identifier and common name of the Association.

Type	N	Cluster	Association
Marsh	2	1	CEGL003924 - Seaside-tansy Tidal Shrub Flat
Hummock	5	2	CEGL007813 - Southern Red-cedar - Live Oak - Cabbage Palmetto Marsh Hammock
Marsh	5	3	CEGL002278 - Salt Flat (Swampfire Type)
Marsh	2	4	CEGL008742 - South Atlantic-Gulf Coast Black Needlerush Salt Marsh
Marsh	15	5	CEGL004191 - Southern Atlantic Coast Salt Marsh
Forest	4	6	CEGL004864 - Ruderal Maritime Slash Pine Woodland
Forest	6	7	CEGL004658 - Maritime Slash Pine - Longleaf Pine Upland Flatwood
Forest	3	8	CEGL004658 - Maritime Slash Pine - Longleaf Pine Upland Flatwood
Forest	2	9	CEGL004747 - Pignut Hickory - Carolina Basswood - Southern Sugar Maple/Spotted Wakerobin Forest
Forest	5	10	CEGL007726 - Southeastern Coastal Plain Ruderal Sweetgum - Oak - Loblolly Pine Forest
Forest	5	11	CEGL007032 - Maritime Live Oak Hammock
Forest	3	12	CEGL007027 - Atlantic Coast Maritime Evergreen Forest

Several environmental variables were significantly related ($p < 0.05$) to the variation in species composition in the NMDS ordination space (Table 2, Figure 3). Specifically, total exchange capacity and salinity loaded negatively onto NMDS 1, while percentage sand loaded positively on NMDS 1. Collectively this suggests the compositional gradient that separates marsh sites (clusters 1, 3, 4 and 5) from hummocks (cluster 2) and forest types (remaining clusters) along NMDS 1 is related to salinity and soil texture differences. Soil pH was strongly positively related to NMDS 2, along with percentage silt and to a lesser degree salinity (Table 2, Figure 3), largely representing an acidity gradient. The compositional gradient along NMDS 3 is related to organic matter and elevation, both of which decrease along this axis. The marsh clusters formed more distinct groupings due to the low degree of compositional overlap, except for cluster 3, which was more compositionally variable, yet still distinct from other marsh types (Figure 3). The forest sites were more species rich and there was considerably more compositional overlap between forest clusters (Figure 3). Overall, salinity, elevation, and TEC explained the most variation in composition across the 3-dimensional ordination space (Table 2). As expected, salinity was considerably higher and elevation was considerably lower in the marsh types relative to the forest types (Figures 3, 4).

Cluster 1 was assigned to the *Borrichia frutescens* / (*Spartina patens*, *Juncus roemerianus*) Saline Shrubland Association (CEGL003924) (Figure 5). This saline shrubland occurs along marsh edges in bands or in tidal flats and is comprised of a variety of salt-adapted species but is primarily dominated by *Borrichia frutescens* (USNVC 2025). Two plots representing this type were located along the upper marsh edge at the transition between salt marsh and the hummock / forest edge or occurred as isolated pockets within salt marshes and salt flats at slightly higher elevation (Figure 6). *Borrichia frutescens* and *Juncus roemerianus* were the dominant species with low cover of other typical salt flat species, such as *Salicornia ambigua* and *Sporobolus virginicus* (Table 3). Relative to other marsh sites, plots of this type had low salinity and species richness and were higher in elevation and pH (Figure 4).

Cluster 2 was assigned to the *Juniperus virginiana* var. *silicicola* - (*Quercus virginiana*, *Sabal palmetto*) Forest Association (CEGL007813) (Figure 5). This is a saline influenced hummock community, which occurs as small islands within salt marsh communities (USNVC 2025). Elevated above the marsh surface, hummocks can support tree species, but inundation is still an influential process, so the woody species present are typically salt tolerant. The canopy of this Association ranges from relatively open to closed, is usually stunted by salt spray, and dominated by *Juniperus silicicola* with lesser amount of *Quercus virginiana* and *Sabal palmetto*. Various marsh species are found in the herbaceous layer (USNVC 2025). The five sites making up this cluster had an open canopy of *Juniperus silicicola* with some stunted *Quercus virginiana* (Table 3). *Ilex vomitoria* was the most constant and abundant species in the mid-story/shrub layer. *Juncus roemerianus* and *Borrichia frutescens* were the most constant and abundant species in the herbaceous layer, although *Spartina patens* and *Sporobolus virginicus* were also present. Salinity was variable and low overall, while elevation was high relative to other marsh types (Figure 4). It was also the most species rich of the marsh types with seven species per 100 m^2.

Cluster 3 was assigned to the *Sarcocornia pacifica* - (*Batis maritima*, *Distichlis spicata*) Saline Dwarf-shrubland Association (CEGL002278) (Figure 5). This hypersaline salt flat/salt panne association is dominated by salt-tolerant succulent species. High salinity conditions occur due to tidal flooding of low marsh flats or high marsh depressions where seawater can accumulate and then evaporate. Ranging along the southern Atlantic coast, *Sarcocornia pacifica* is the primary diagnostic species of this assemblage, while other species such as *Batis maritima*, *Salicornia* spp., *Borrichia frutescens*, *Distichlis spicata*, and stunted *Spartina alterniflora* are often present (USNVC 2025). Similarly to cluster 1, this type was mapped mostly along the upper marsh edge, a distribution consistent with the type description (Figure 6). There were five sites that comprised this cluster, with *Salicornia ambigua* and *Batis maritima* as

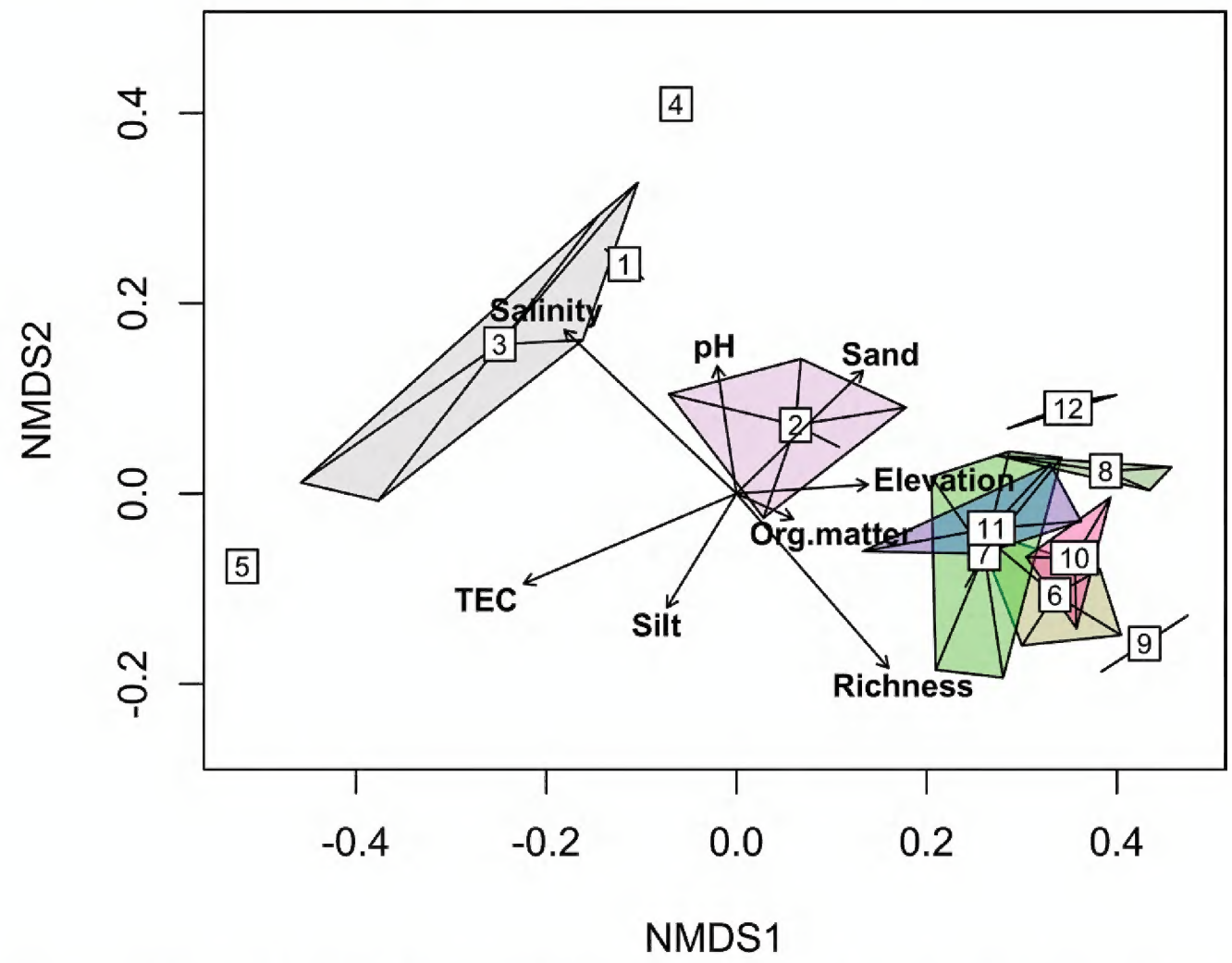

Figure 3. Non-metric multidimensional scaling (NMDS) ordination of all plots based on abundance-weighted Bray-Curtis dissimilarity. Final cluster membership is shown as colored polygons labeled with cluster numbers whose vertices are the sites belonging to that cluster (ordispider function, vegan package in R, Oksanen et al. 2022): marsh types (clusters 1, 3, 4, and 5), hummocks (cluster 2), and forest types (clusters 6–12). Stress of the NMDS ordination after 100 iterations was 0.04. Environmental vectors that were significantly related ($p < 0.05$) to the NMDS axes are overlayed. Vector length is scaled by the correlation coefficient values. TEC = total exchange capacity, Org. matter = organic matter. Cluster 1 = saline shrubland, cluster 2 = hummock, cluster 3 = salt flat, cluster 4 = brackish marsh, cluster 5 = salt marsh, cluster 6 = open pine woodland, cluster 7 = pine woodland with maritime influence, cluster 8 = pine forest with maritime influence, cluster 9 = temperate deciduous forest, cluster 10 = mixed forest, cluster 11 = maritime forest type 1, and cluster 12 = maritime forest type 2.

Table 2. Loadings of each environmental variable on the NMDS axes, and the associated R^2 and p-values. Variables were overlaid using the "envfit" function (package 'vegan') in R (Oksanen et al. 2022). TEC = total exchange capacity, Org.matter = organic matter.

	NMDS1	NMDS2	NMDS3	R^2	p-value	
TEC	-0.90168	-0.38155	-0.20346	0.682264	0.001	***
pH	-0.14986	0.987724	-0.04409	0.204504	0.009	**
Org.matter	0.352972	-0.15763	-0.92226	0.316105	0.001	***
Silt	-0.47583	-0.77979	-0.40684	0.261385	0.001	***
Sand	0.650888	0.631078	0.422002	0.463891	0.001	***
Richness	0.57806	-0.66379	0.474577	0.848502	0.001	***
Salinity	-0.67649	0.642602	0.359748	0.794236	0.001	***
Elevation	0.535244	0.037822	-0.84385	0.740365	0.001	***

Signif. codes: 0 '***' 0.001 '**' 0.01 '*' 0.05 '.' 0.1 ' ' 1.

the most constant and abundant species (Table 3). Even these dominant species were relatively sparse, with large patches of unvegetated, saturated, sandy substrate. The composition and environmental conditions of these sites were consistent with the USNVC type concept and its documented range. Salinity was variable but on average it was among the most saline types that we surveyed (Figure 4). Differences in salinity among plots representing this type were likely driven by differences in distance from the coast. Consistent with high salinity, this type occurs at low elevation: only cluster 5 (salt marsh) was lower in elevation. Species richness was low with four species per 100 m^2. The lowest organic matter was observed in this type (Figure 4).

Cluster 4 was assigned to *Juncus roemerianus* South Atlantic and Gulf Coastal Salt Marsh - (CEGL008742) (Figure 5). This is a high marsh association that is typically a monospecific community of *Juncus roemerianus* that is widely distributed along the South Atlantic and Gulf Coasts (USNVC 2025). The two sites that we surveyed

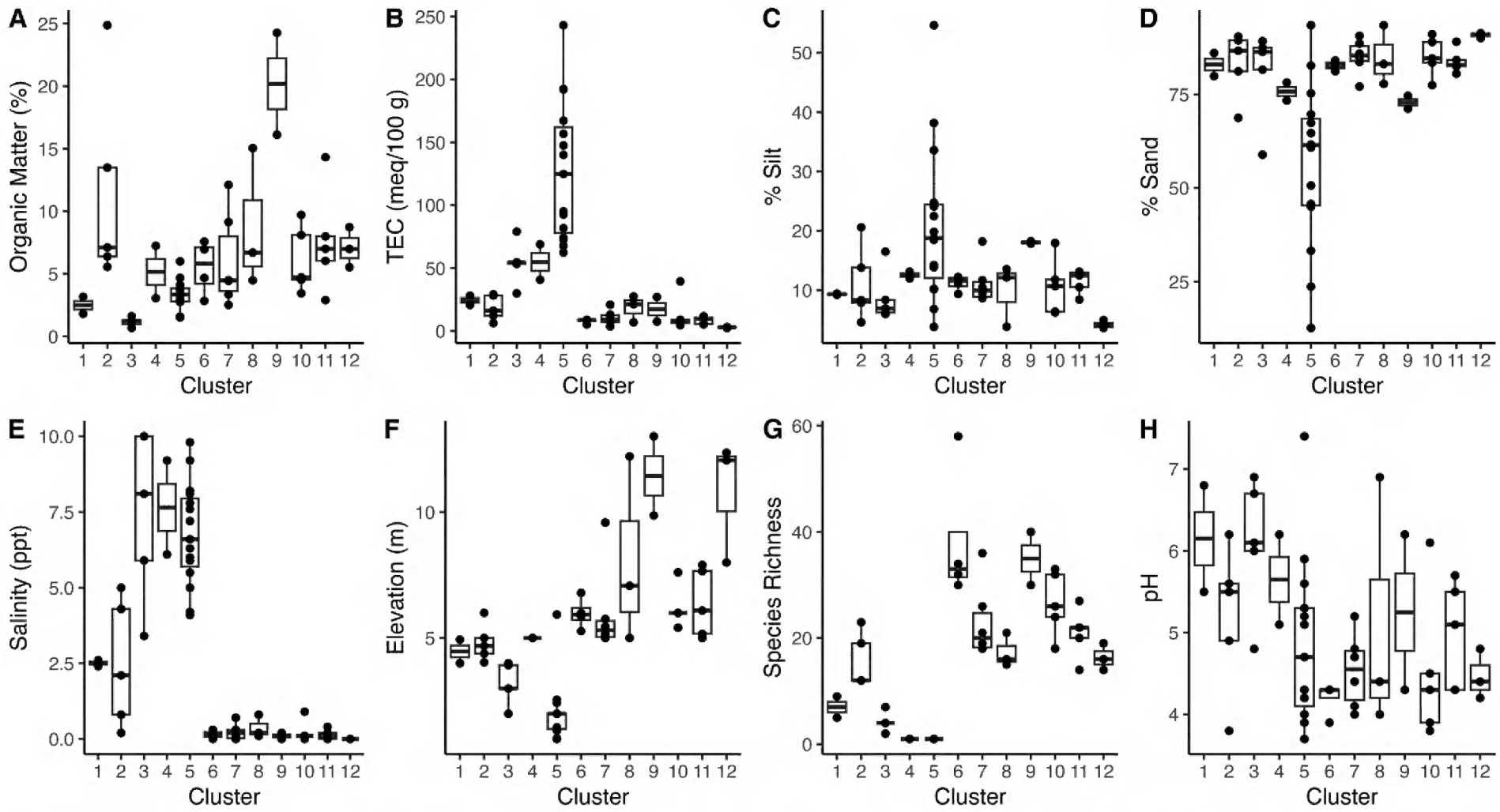

Figure 4. Boxplots of environmental variables for the 12 clusters. Boxplots display the distributions of soil nutrient and texture, salinity (parts per thousand), elevation (meters), and species richness for plots assigned to each cluster. TEC = total exchange capacity (milliequivalents / 100 g). Cluster 1 = saline shrubland, cluster 2 = hummock, cluster 3 = salt flat, cluster 4 = brackish marsh, cluster 5 = salt marsh, cluster 6 = open pine woodland, cluster 7 = pine woodland with maritime influence, cluster 8 = pine forest with maritime influence, cluster 9 = temperate deciduous forest, cluster 10 = mixed forest, cluster 11 = maritime forest type 1, and cluster 12 = maritime forest type 2.

consistent with this composition (Table 3) were in high marsh locations existing in low lying depressions along forest edges where tidal flushing is less frequent and standing water is always present (even at low tide) (Figure 6). This cluster, along with cluster 5, are the most species-poor of the marsh types – all were dominated by a single species (*Juncus roemarianus*). This type had the highest elevation of the marsh types and among the highest pH (Figure 4). The salinity of this type was high because there is less tidal exchange and salts brought in by occasional flooding or storm tides accumulate in the soil.

The final marsh site cluster, cluster 5, was assigned to the *Spartina alterniflora* South Atlantic Salt Marsh Association (CEGL004191) (Figure 5). As the name suggests, this is the dominant low salt marsh vegetation assemblage of the South Atlantic Coast, characterized by *Spartina alterniflora* that experiences regular tidal flooding (USNVC 2025). This was the most extensive Association on MCRD-PI (Table 3; Figure 6). Fifteen of our marsh sites were consistent with this type, all of which were monospecific communities of *S. alterniflora* (Table 3). Vegetation height was variable, with taller plants in soft marsh substrate that experiences more inundation. These sites exhibited variability in salinity but were overall intermediate relative to other marsh types (Figure 4). Total exchange capacity and pH were also quite variable. Overall, pH was low relative to other marsh types and total exchange capacity was the highest relative to all other types. As expected, elevation was the lowest in this type.

The first forest cluster, cluster 6, was assigned to the *Pinus elliottii* Ruderal Maritime Woodland Association (CEGL004864) (Figure 5). This type is characterized as a successional community, likely forming after canopy-opening disturbances on barrier islands. It is dominated by an overstory of *Pinus elliottii*, with some sparse *Sabal palmetto* and a ruderal, maritime-influenced herbaceous and shrub layer (USNVC 2025). The four sites that were grouped into this woodland cluster had open canopies dominated by *Pinus elliottii* with a high constancy of *Liquidambar styraciflua*, although relatively low cover (Table 3). The mid-story shrub layer was relatively sparse (mean shrub cover = 28.5%), composed primarily of *Morella cerifera* with lesser amounts of *Ilex vomitoria* and the invasive *Triadica sebifera*. The understories contained various ruderal species (e.g., *Andropogon virginicus*, *Eupatorium capillifolium*, *Paspalum* spp., and *Rubus* spp.). These sites were among some of the most species rich in the herbaceous layer, with one site that was far more diverse than any others (Figure 4). Most of the forest sites had low salinity and the sites in this cluster were consistent with that range (Figure 7). This type occurred at slightly higher elevations than the high marsh clusters previously described (Figure 4). pH was also among the lowest of any of the types. All of the sites within this type were subject to canopy thinning and most to prescribed fire, reflected by the low canopy cover (Figure 7). This likely promoted the diverse herbaceous layer of disturbance-adapted species due to increases in light availability.

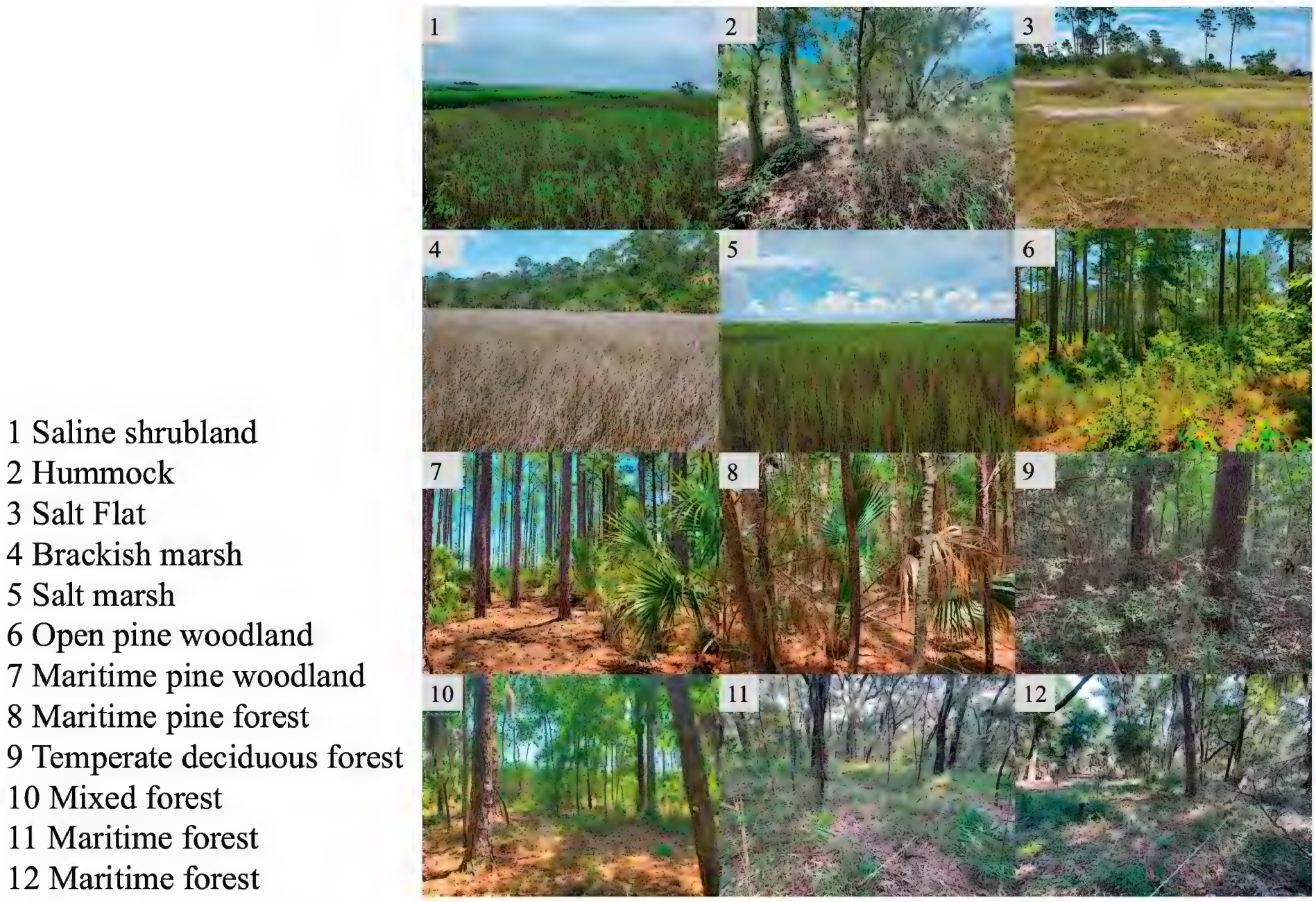

Figure 5. Images of the 12 vegetation types that were identified from quantitative analysis of vegetation plot data. The cluster number and the short-hand vegetation type name are provided to the left. See Table 1 for the USNVC Associations these clusters represent.

Cluster 7 was assigned to the *Pinus elliottii* - (*Pinus palustris*) / *Ilex vomitoria* - *Serenoa repens* - *Morella cerifera* Woodland Association (CEGL004658) (Figure 5). This is a maritime-influenced *Pinus elliottii* woodland that can sometimes contain *Pinus palustris*, which occurs on barrier islands and other areas very close to the coast. The subcanopy can contain maritime *Quercus* species with a shrub layer of *Ilex vomitoria* and *Morella cerifera*. The herbaceous layer is typically sparse and species-poor (USNVC 2025). The six plots in this cluster had overstories of both *Pinus elliottii* and *Pinus taeda*. *Pinus taeda* is not mentioned in the type description, but these sites otherwise fit this association well, despite lacking *P. palustris*, which is absent on MCRDPI. A very sparse subcanopy of primarily *Quercus virginiana* was present in most sites (Figure 7). The shrub and herb layers are consistent with the USNVC type description (Table 3). Species richness was intermediate to low relative to other forest types (Figure 4). Most of the sites were similar to other forest types with regard to salinity apart from one site with high salinity (Figure 7). This type had the lowest elevation of all the forest types but was slightly higher in elevation than all marsh types (Figures 4, 7).

Cluster 8 was assigned to the same association as cluster 7, the *Pinus elliottii* - (*Pinus palustris*) / *Ilex vomitoria* - *Serenoa repens* - *Morella cerifera* Woodland Association (CEGL004658) (Figure 5). These clusters are floristically similar but likely grouped separately due to differences in canopy cover. Cluster 8 has a dense canopy dominated by *Pinus elliottii*, whereas cluster 7 has a sparser canopy of both *P. elliottii* and *P. taeda* (Figure 7). There was otherwise a high compositional similarity between the clusters (Table 3, Figure 3). Therefore, we classified them as subtypes of the same Association - cluster 7 represents the woodland subtype and cluster 8 represents the forest subtype. This is consistent with the type description, which recognizes variation in canopy openness and canopy structure (USNVC 2025). We also mapped them at the subtype level since the structural differences between the canopies of these types are recognizable from aerial imagery and may be useful for management and conservation decisions. All three sites within cluster 8 had relatively sparse shrub layers (mean shrub cover = 23.3%) made up of *Ilex vomitoria* and *Morella cerifera* and somewhat depauperate, ruderal herbaceous layers (Table 3). These sites were among some of the most species-poor of the forest sites (Figure 4). Salinity at one of the sites was noticeably higher than the others, but, overall, salinity of this cluster fell within the range of other forest types (Figure 7). Total exchange capacity was high relative to other forest types (Figure 7), while elevation was variable, spanning the range observed among other forest types (Figure 4).

Table 3. Species constancy table. The table shows the constancy of species that are present in at least 50% of the sites assigned to each cluster and the average percentage cover (e.g., the average of the midpoint cover codes, including sites that the species was not present in) of that species ("con" = constancy, "cov" = cover). We considered diagnostic species (shown in gray) to be those that had 50% constancy or greater and occurred with an average cover of 2% or greater.

Species	Con 1	Cov 1	Con 2	Cov 2	Con 3	Cov 3	Con 4	Cov 4	Con 5	Cov 5	Con 6	Cov 6	Con 7	Cov 7	Con 8	Cov 8	Con 9	Cov 9	Con 10	Cov 10	Con 11	Cov 11	Con 12	Cov 12
Juncus roemerianus	1	85	0.8	21	.	.	1	91	.	.	.	.	.	.	.	.	.	.	.	.	.	.	.	.
Borrichia frutescens	1	28	0.8	14	0.6	9.7	.	.	.	.	.	.	.	.	.	.	.	.	.	.	.	.	.	.
Sporobolus virginicus	1	2.5	.	.	.	.	.	.	.	.	.	.	.	.	.	.	.	.	.	.	.	.	.	.
Salicornia ambigua	1	2	.	.	0.8	3.8	.	.	.	.	.	.	.	.	.	.	.	.	.	.	.	.	.	.
Solidago mexicana	1	0.3	.	.	.	.	.	.	.	.	.	.	.	.	.	.	.	.	.	.	.	.	.	.
Distichlis spicata	0.5	0.8	0.6	2.3	.	.	.	.	.	.	.	.	.	.	.	.	.	.	.	.	.	.	.	.
Juniperus silicicola	0.5	0.3	0.8	16	.	.	.	.	.	.	0.5	0.2	0.5	0.4	.	.	0.5	0.1	0.8	0.4	0.6	0.8	.	.
Batis maritima	0.5	0.1	.	.	0.8	5.8	.	.	.	.	.	.	.	.	.	.	.	.	.	.	.	.	.	.
Salicornia bigelovii	0.5	0.1	.	.	.	.	.	.	.	.	.	.	.	.	.	.	.	.	.	.	.	.	.	.
Ilex vomitoria	.	.	1	4	.	.	.	.	.	.	1	2.8	1	13	1	9.5	1	50	1	27	1	13	1	48
Quercus virginiana	.	.	0.8	22	.	.	.	.	.	.	0.8	1	0.7	6.7	.	.	.	.	0.6	19	1	44	1	7.2
Tillandsia usneoides	.	.	0.8	7.4	.	.	.	.	.	.	.	.	0.8	0.8	0.7	1.2	1	2	1	8.1	1	6.3	1	46
Sabal palmetto	.	.	0.8	4.4	.	.	.	.	.	.	0.5	0.4	1	4.2	1	5.5	1	20	1	1.1	1	26	1	2.8
Baccharis angustifolia	.	.	0.8	1.4	.	.	.	.	.	.	.	.	.	.	.	.	.	.	.	.	.	.	.	.
Fimbristylis castanea	.	.	0.6	1.5	.	.	.	.	.	.	.	.	.	.	.	.	.	.	.	.	.	.	.	.
Pinus elliottii	.	.	0.6	1.1	.	.	.	.	.	.	1	45	0.5	23	1	62	.	.	0.8	17	0.6	3.1	.	.
Baccharis halimifolia	.	.	0.6	0.3	.	.	.	.	.	.	0.8	2	0.7	1.5	.	.	.	.	.	.	.	.	.	.
Spartina alterniflora	.	.	.	.	.	.	.	.	1	39	.	.	.	.	.	.	.	.	.	.	.	.	.	.
Morella cerifera	.	.	.	.	.	.	.	.	.	.	1	6.8	1	8.3	1	6.2	1	1.5	1	12	0.6	0.6	.	.
Triadica sebifera	.	.	.	.	.	.	.	.	.	.	1	2.3	1	1.9	.	.	.	.	1	2.3	0.6	0.4	.	.
Andropogon virginicus	.	.	.	.	.	.	.	.	.	.	1	1.5	0.7	0.1	.	.	0.5	0.1	.	.	.	.	.	.
Quercus nigra	.	.	.	.	.	.	.	.	.	.	1	0.5	1	0.2	0.7	2.7	0.5	0.1	1	15	0.8	2	.	.
Hypericum hypericoides	.	.	.	.	.	.	.	.	.	.	1	0.5	.	.	.	.	0.5	0.3	0.6	0.1	.	.	.	.
Liquidambar styraciflua	.	.	.	.	.	.	.	.	.	.	0.8	21	.	.	.	.	1	23	1	9.3	.	.	.	.
Nyssa sylvatica	.	.	.	.	.	.	.	.	.	.	0.8	2	.	.	.	.	0.5	0.1	0.6	0.2	.	.	.	.
Rubus argutus	.	.	.	.	.	.	.	.	.	.	0.8	1.1	0.5	0.2	1	0.2	0.5	0.3	0.6	0.8	0.6	0.3	.	.
Rubus pensilvanicus	.	.	.	.	.	.	.	.	.	.	0.8	1.1	.	.	.	.	.	.	.	.	.	.	.	.
Dichanthelium portoricense	.	.	.	.	.	.	.	.	.	.	0.8	0.6	.	.	.	.	.	.	0.8	0.4	.	.	.	.
Paspalum sp.	.	.	.	.	.	.	.	.	.	.	0.8	0.6	.	.	.	.	.	.	.	.	.	.	.	.
Campsis radicans	.	.	.	.	.	.	.	.	.	.	0.8	0.4	0.5	0.3	0.7	0.7	.	.	0.6	0.8	.	.	.	.
Juncus dichotomus	.	.	.	.	.	.	.	.	.	.	0.8	0.4	.	.	.	.	.	.	.	.	0.6	0.3	.	.
Panicum virgatum	.	.	.	.	.	.	.	.	.	.	0.8	0.4	.	.	.	.	.	.	.	.	.	.	.	.
Dichanthelium scoparium	.	.	.	.	.	.	.	.	.	.	0.8	0.3	.	.	.	.	.	.	.	.	.	.	.	.
Eupatorium capillifolium	.	.	.	.	.	.	.	.	.	.	0.8	0.3	.	.	.	.	.	.	.	.	.	.	.	.
Rhexia mariana var. *mariana*	.	.	.	.	.	.	.	.	.	.	0.8	0.3	.	.	.	.	.	.	.	.	.	.	.	.
Smilax bona-nox	.	.	.	.	.	.	.	.	.	.	0.8	0.3	0.7	0.9	1	1.5	1	0.5	1	1.3	0.8	1	.	.
Parthenocissus quinquefolia	.	.	.	.	.	.	.	.	.	.	0.8	0.1	0.5	0.3	1	0.4	1	2.5	.	.	0.8	1	.	.
Prunus serotina	.	.	.	.	.	.	.	.	.	.	0.8	0.1	0.5	0.2	.	.	1	0.3	.	.	0.6	0.1	.	.
Paspalum setaceum	.	.	.	.	.	.	.	.	.	.	0.5	2	.	.	.	.	0.5	0.3	.	.	.	.	.	.
Andropogon cretaceus	.	.	.	.	.	.	.	.	.	.	0.5	0.8	.	.	.	.	.	.	.	.	.	.	.	.
Callicarpa americana	.	.	.	.	.	.	.	.	.	.	0.5	0.5	.	.	.	.	1	0.5	.	.	.	.	.	.
Dichanthelium villosissimum	.	.	.	.	.	.	.	.	.	.	0.5	0.3	.	.	.	.	.	.	.	.	.	.	.	.
Pinus taeda	.	.	.	.	.	.	.	.	.	.	0.5	0.3	0.7	24	.	.	0.5	0.3	0.6	15	.	.	.	.
Smilax glauca	.	.	.	.	.	.	.	.	.	.	0.5	0.3	.	.	.	.	0.5	0.3	1	0.3	.	.	.	.
Vitis rotundifolia	.	.	.	.	.	.	.	.	.	.	0.5	0.3	.	.	0.7	2.3	0.5	0.3	0.8	0.8	.	.	1	4.2
Acer rubrum	.	.	.	.	.	.	.	.	.	.	0.5	0.2	.	.	.	.	0.5	1.8	.	.	.	.	.	.
Rhus copallinum	.	.	.	.	.	.	.	.	.	.	0.5	0.2	.	.	.	.	.	.	.	.	.	.	.	.
Erechtites hieraciifolius	.	.	.	.	.	.	.	.	.	.	0.5	0.1	.	.	.	.	.	.	.	.	.	.	.	.
Houstonia tenuifolia	.	.	.	.	.	.	.	.	.	.	0.5	0.1	.	.	.	.	.	.	.	.	.	.	.	.
Toxicodendron radicans	.	.	.	.	.	.	.	.	.	.	.	.	.	.	1	1	1	2.5	0.8	1.3	0.6	0.2	.	.
Galium orizabense	.	.	.	.	.	.	.	.	.	.	.	.	.	.	0.7	0.3	1	0.3	.	.	.	.	.	.
Vitis sp.	.	.	.	.	.	.	.	.	.	.	.	.	.	.	0.7	0.1	0.5	1.8	.	.	.	.	.	.
Quercus pagoda	.	.	.	.	.	.	.	.	.	.	.	.	.	.	.	.	1	50	.	.	.	.	.	.
Fraxinus pennsylvanica	.	.	.	.	.	.	.	.	.	.	.	.	.	.	.	.	1	11	.	.	.	.	.	.
Morus rubra	.	.	.	.	.	.	.	.	.	.	.	.	.	.	.	.	1	7.5	.	.	.	.	.	.

Species	Con 1	Cov 1	Con 2	Cov 2	Con 3	Cov 3	Con 4	Cov 4	Con 5	Cov 5	Con 6	Cov 6	Con 7	Cov 7	Con 8	Cov 8	Con 9	Cov 9	Con 10	Cov 10	Con 11	Cov 11	Con 12	Cov 12
Arisaema triphyllum	.	.	.	.	.	.	.	.	.	.	.	.	.	.	.	.	1	4	.	.	.	.	.	.
Bignonia capreolata	.	.	.	.	.	.	.	.	.	.	.	.	.	.	.	.	1	2.5	.	.	.	.	.	.
Ligustrum sinense	.	.	.	.	.	.	.	.	.	.	.	.	.	.	.	.	1	2	.	.	.	.	.	.
Celtis laevigata	.	.	.	.	.	.	.	.	.	.	.	.	.	.	.	.	1	1.8	.	.	.	.	.	.
Oplismenus setarius	.	.	.	.	.	.	.	.	.	.	.	.	.	.	.	.	1	1	.	.	.	.	.	.
Aesculus pavia	.	.	.	.	.	.	.	.	.	.	.	.	.	.	.	.	1	0.5	.	.	.	.	.	.
Lonicera japonica	.	.	.	.	.	.	.	.	.	.	.	.	.	.	.	.	1	0.3	.	.	.	.	.	.
Ambrosia artemisiifolia	.	.	.	.	.	.	.	.	.	.	.	.	.	.	.	.	1	0.1	.	.	.	.	.	.
Magnolia grandiflora	.	.	.	.	.	.	.	.	.	.	.	.	.	.	.	.	0.5	31	.	.	.	.	0.7	2.5
Dichanthelium laxiflorum	.	.	.	.	.	.	.	.	.	.	.	.	.	.	.	.	0.5	1.8	.	.	.	.	0.7	1.3
Carya glabra	.	.	.	.	.	.	.	.	.	.	.	.	.	.	.	.	0.5	19	.	.	.	.	1	5.9
Arundinaria tecta	.	.	.	.	.	.	.	.	.	.	.	.	.	.	.	.	0.5	3.8	.	.	.	.	.	.
Elaeagnus umbellata	.	.	.	.	.	.	.	.	.	.	.	.	.	.	.	.	0.5	1.8	.	.	.	.	.	.
Asplenium platyneuron	.	.	.	.	.	.	.	.	.	.	.	.	.	.	.	.	0.5	0.3	.	.	.	.	.	.
Dichanthelium sp.	.	.	.	.	.	.	.	.	.	.	.	.	.	.	.	.	0.5	0.3	.	.	.	.	.	.
Juncus coriaceus	.	.	.	.	.	.	.	.	.	.	.	.	.	.	.	.	0.5	0.3	.	.	.	.	.	.
Pleopeltis polypodioides	.	.	.	.	.	.	.	.	.	.	.	.	.	.	.	.	0.5	0.3	.	.	.	.	.	.
Rubus sp.	.	.	.	.	.	.	.	.	.	.	.	.	.	.	.	.	0.5	0.3	.	.	.	.	.	.
Sanicula canadensis	.	.	.	.	.	.	.	.	.	.	.	.	.	.	.	.	0.5	0.3	.	.	.	.	.	.
Boehmeria cylindrica	.	.	.	.	.	.	.	.	.	.	.	.	.	.	.	.	0.5	0.1	.	.	.	.	.	.
Ilex opaca	.	.	.	.	.	.	.	.	.	.	.	.	.	.	.	.	0.5	0.1	.	.	.	.	.	.
Onoclea sensibilis	.	.	.	.	.	.	.	.	.	.	.	.	.	.	.	.	0.5	0.1	.	.	.	.	.	.
Quercus hemisphaerica	.	.	.	.	.	.	.	.	.	.	.	.	.	.	.	.	.	.	.	.	.	.	1	63
Vaccinium arboreum	.	.	.	.	.	.	.	.	.	.	.	.	.	.	.	.	.	.	.	.	.	.	1	8.2
Persea borbonia	.	.	.	.	.	.	.	.	.	.	.	.	.	.	.	.	.	.	.	.	.	.	1	7.5
Gelsemium sempervirens	.	.	.	.	.	.	.	.	.	.	.	.	.	.	.	.	.	.	0.6	1.1	.	.	1	0.5
Pinus glabra	.	.	.	.	.	.	.	.	.	.	.	.	.	.	.	.	.	.	.	.	.	.	0.7	13

Cluster 9 was assigned to the *Carya glabra - Tilia americana* var. *caroliniana - Acer floridanum / Trillium maculatum* Forest Association (CEGL004747) (Figure 5). This is a mesic to dry-mesic calcareous influenced forest type of the South Carolina Outer Coastal Plain with a diverse overstory of deciduous species, including *Acer floridanum*, *Carya glabra*, *Celtis laevigata*, *Fraxinus americana*, *Tilia americana* var. *caroliniana*, and *Quercus pagoda*, among others. The shrub and herbaceous layers are dominated by calciphylic species, such as *Aesculus pavia*, *Morus rubra*, and *Sabal minor* (USNVC 2025). The presence of this type was relatively restricted, occurring as a few isolated stands along the southern edge of the main infrastructure of MCRDPI (Figure 6). Both sites in this cluster had significant *Quercus pagoda* overstory cover and some *Fraxinus pennsylvanica* and *Morus rubra* in the subcanopy. Other tree species documented in plots that are consistent with the type description include *Celtis laevigata* and *Carya glabra* (Table 3). Other constant and abundant tree species in plots were *Liquidambar styraciflua*, *Magnolia grandiflora*, *Aesculus pavia*, and *Sabal palmetto*. The mid-story layer was dominated by *Ilex vomitoria* and *Morella cerifera*. *Arisaema triphyllum*, *Bignonia capreolata*, *Callicarpa americana*, *Galium orizabense*, *Lonicera japonica*, *Oplismenus setarius*, *Smilax bona-nox*, and *Toxicodendron radicans* were consistently found in the diverse understory layer (Table 3). There are several other species described in the type concept that were not present in these sites, most notably *Tilia americana* var. *caroliniana* and *Acer floridanum*. Otherwise, our plots fit the type well. This is a diverse Association which requires additional data to better describe its occurrences (USNVC 2025). There is certainly evidence of calcareous influence in one site, while the other had calcium levels comparable to that of other sites (Figure 7). This type was among the most species rich and had the highest canopy cover (Figures 4, 7). It also had the highest elevation and organic matter (Figure 4).

Cluster 10 was assigned to the *Liquidambar styraciflua - Quercus nigra - Pinus taeda / Vaccinium elliottii - Morella cerifera* Ruderal Forest Association (CEGL007726) (Figure 5). This forest type develops in upland areas after the cessation of agriculture or other significant disturbances. It has a canopy co-dominated by *Quercus* spp. (especially *Q. nigra* and *Q. phellos*) and *Liquidambar styraciflua*. *Pinus taeda* may or may not be present and can achieve high cover when it occurs. The subcanopy contains various hardwoods, such as *Nyssa sylvatica*, *Liriodendron tulipifera*, *Acer rubrum*, and *Prunus serotina*. Vine species are often present, including *Vitis rotundifolia*, *Gelsemium sempervirens*, *Toxicodendron radicans*, and *Smilax* spp. The shrub layer is sparse, but *Morella cerifera* can reach high abundance in some cases. The herb layer is moderately developed and primarily dominated by graminoids (USNVC 2025). The five sites in this cluster were very consistent with this description. Most sites had a sparse canopy of mature *P. taeda* and *P. elliottii*, and a scattered canopy and subcanopy dominated by *Liquidambar styraciflua*, *Q. nigra*, and *Q. virginiana* (Table 3). *Ilex vomitoria* and *Morella cerifera* were constant and abundant species in the shrub layer. All

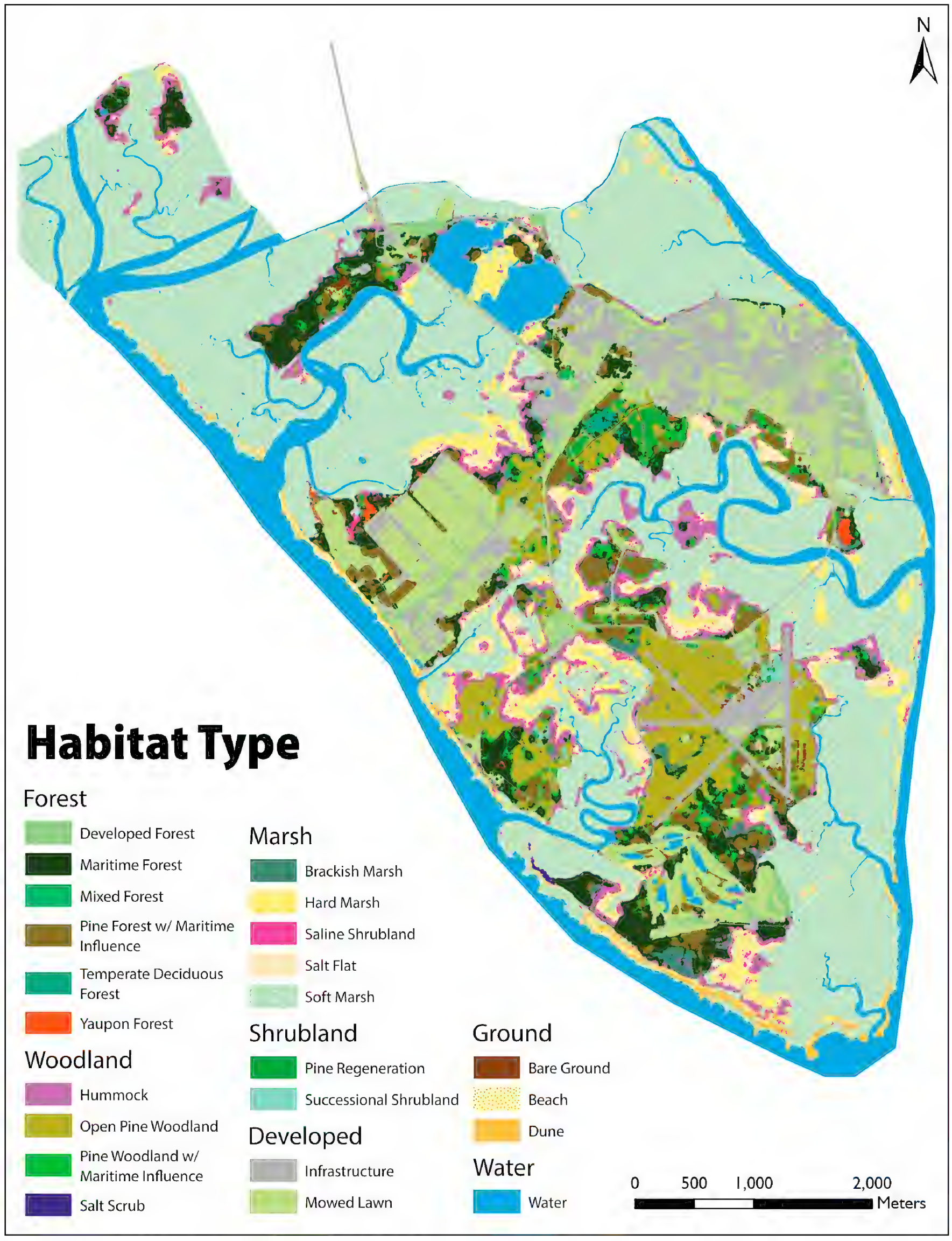

Figure 6. Vegetation map of MCRDPI for 2022 containing 23 land cover types. Twelve vegetation types were identified through quantitative analysis of vegetation plot data and were cross-walked onto USNVC Associations: saline shrubland (cluster 1, CEGL003924), hummock (cluster 2, CEGL007813), salt flat (cluster 3, CEGL002278), brackish marsh (cluster 4, CEGL008742), soft marsh and hard marsh (cluster 5, CEGL004191), open pine woodland (cluster 6, CEGL004864), pine woodland w/ maritime influence (cluster 7, CEGL004658), pine forest w/ maritime influence (cluster 8, CEGL004658), temperate deciduous forest (cluster 9, CEGL004747), mixed forest (cluster 10, CEGL007726), and maritime forest represented by cluster 11 (CEGL007032) and cluster 12 (CEGL007027). The two maritime forest types could not be distinguished in our mapping effort because they had very similar spectral signatures and were mapped as a single maritime forest class. Additional mapped land cover types (N = 11) not captured by vegetation plots include: bare ground, beach, developed forest, dune, infrastructure, mowed lawn, pine regeneration, salt scrub, successional shrubland, water, and yaupon forest.

the vine species listed above were present in most sites. The herbaceous layer was sparse covered and included several species present that were mentioned in the description. The species richness in this type was variable, ranging from low to moderate relative to other forest types (Figure 4). Elevation was generally low relative to other forest types. Salinity and total exchange capacity were consistent with other forest types except for one outlier site that had the highest salinity and TEC of any forest site (Figure 7). The pH was also quite low (Figure 4) and canopy cover was intermediate relative to other types (Figure 7).

Cluster 11 was assigned to the *Quercus virginiana* - (*Pinus elliottii*, *Sabal palmetto*) / *Persea borbonia* - *Callicarpa americana* Forest Association (CEGL007032) (Figure 5). This maritime forest type occurs at the marsh or ocean edge of barrier islands. More southern occurrences are dominated strongly by *Quercus virginiana* and *Sabal palmetto*, potentially with a component of *Pinus elliottii*. Many other maritime influenced species may be present in this Association (e.g., *Ilex vomitoria*, *Persea borbonia*), and vine species are often an important component (USNVC 2025). Apart from one site, all the sites assigned to this type occurred along the seaward edge of MCRDPI (Figure 6). The five sites in this cluster had a canopy dominated by *Quercus virginiana* and *Sabal palmetto* (Table 3). *Ilex vomitoria* was an important species in the shrub layer and *Tillandsia usneoides* was constant and abundant. Several vine species had high constancy, including *Parthenocissus quinquefolia*, *Smilax bona-nox*, and *Toxicodendron radicans*. The herbaceous layer was poorly developed, which is consistent with the type description. Species richness and elevation were variable, ranging from low to moderate relative to other forest types, with one site of this cluster being one of the most depauperate of the forest sites (Figure 4). Salinity was variable; it was mostly consistent with other forest types, with a few sites displaying slightly elevated levels (Figure 7). Canopy cover was variable as well, ranging from intermediate to high.

Finally, cluster 12 was assigned to the *Quercus virginiana* - *Quercus hemisphaerica* - *Pinus taeda* / *Persea palustris* - *Ilex vomitoria* Forest Association (CEGL007027) (Figure 5). This maritime forest type occurs on stable dunes where the vegetation is often affected by salt spray. *Quercus virginiana* and *Quercus hemisphaerica* are the canopy dominants. Some *Pinus taeda* and *Juniperus silicicola* may also be present. The upper strata are often dense, containing abundant vine species (e.g., *Vitis rotundifolia* and *Gelsemium sempervirens*) and suppressing the herbaceous layer. *Ilex vomitoria* and *Morella cerifera* typically dominate the shrub layer. Other common woody species are *Persea borbonia* and

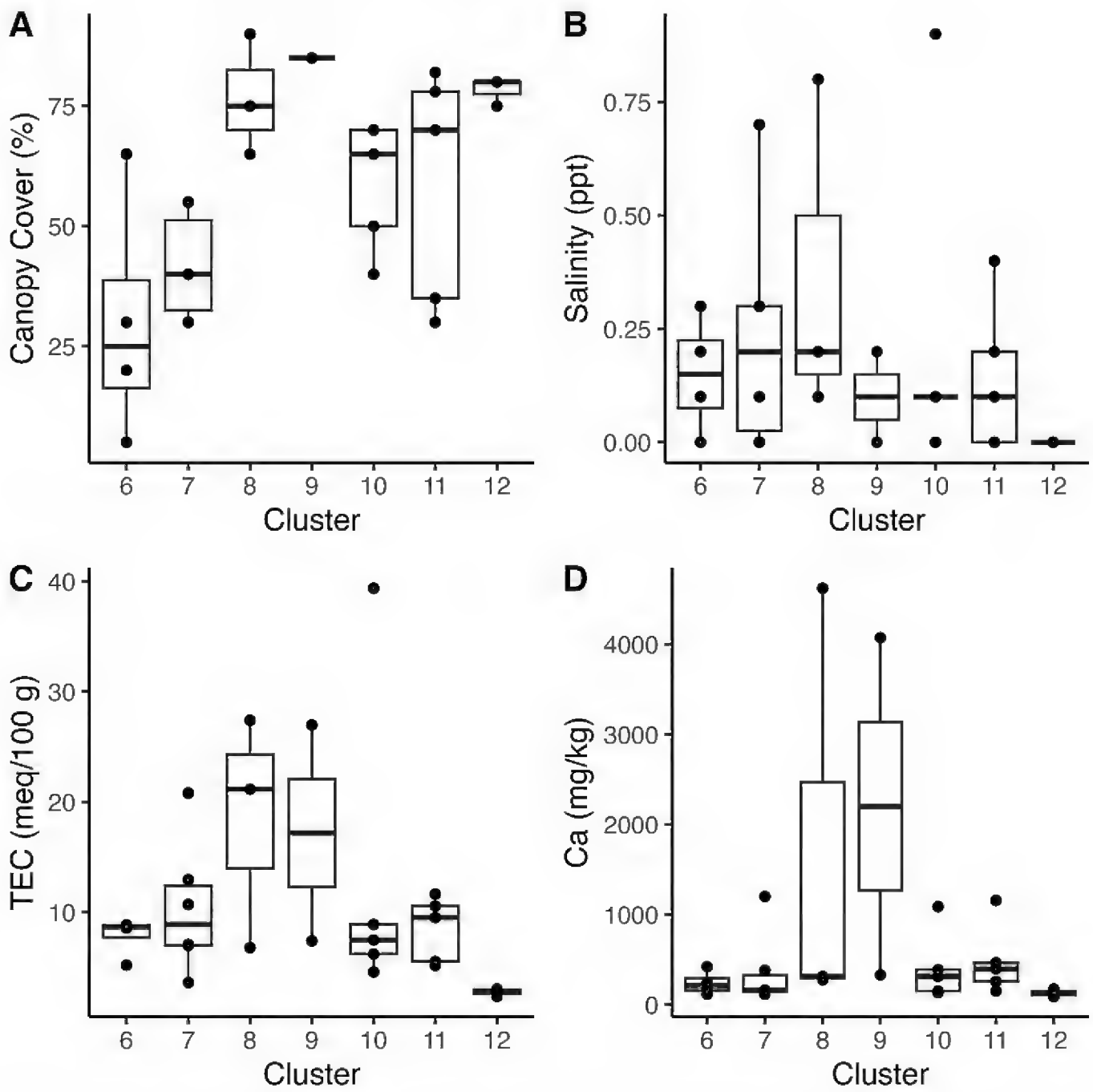

Figure 7. Boxplots displaying the distributions of select environmental variables among the forest clusters. Boxplots show tree canopy cover (A), salinity (B), total exchange capacity (C), and calcium (mg/kg) (D). Cluster 1 = saline shrubland, cluster 2 = hummock, cluster 3 = salt flat, cluster 4 = brackish marsh, cluster 5 = salt marsh, 6 = open pine woodland, 7 = pine woodland with maritime influence, 8 = pine forest with maritime influence, 9 = temperate deciduous forest, 10 = mixed forest, 11 = maritime forest type 1, and 12 = maritime forest type 2.

Zanthoxylum clava-herculis (USNVC 2025). The three sites assigned to cluster 12 were near each other, located on the northern edge of Horse Island (Figure 6). The overstory was dominated by *Quercus hemisphaerica* with lesser amounts of *Quercus virginiana* (Table 3). *Pinus glabra* rather than *Pinus taeda* was present and no *Juniperus silicicola* was identified. All shrubs, vines, and herbs described above were present except for *Zanthoxylum clava-herculis*. *Vaccinium arboreum* and *Persea borbonia* were diagnostic species in the mid-story layer. *Tillandsia usneoides* cover was high. The herb layer was quite depauperate and accordingly, these were among the most species-poor forest sites (Figure 4). Elevation and canopy cover were high overall (Figures 4, 7). This type had the lowest salinity and the sandiest soil (Figures 4, 7). It also had strong compositional affinity to the *Quercus hemisphaerica - Magnolia grandiflora - Carya pallida / Vaccinium arboreum / Chasmanthium sessiliflorum* Forest Association (CEGL004788). However, that Association is described to occur on slopes along rivers and streams, which was not consistent with the occurrences that we surveyed (USNVC 2025). Therefore, we ultimately assigned this cluster to CEGL007027, but our observations may warrant further review of these type concepts.

Vegetation map

The soft and hard marsh classes (dominated by *Spartina alterniflora*, cluster 5) cover 44.4% of the classified area, while all marsh vegetation classes (including salt flats and saline shrublands) collectively cover 49.4% (Table 4). The saline shrubland (cluster 1) and salt flat (cluster 3) classes are high marsh assemblages occurring along the upper marsh boundary (Figure 6), collectively covering 3.4% of the classified area (Table 4). The most dominant forest class is maritime forest (clusters 11 and 12), which covers 5.1% of the classified area (Table 4). The two maritime forest types could not be distinguished in our mapping effort because they were very similar in terms of their spectral signature. Thus, the two types were mapped as a single maritime forest class. The largest continuous forested area on MCRDPI occurs around Page Field, an abandoned airfield used for training purposes (Figure 6). This area is dominated by the open pine woodland class (cluster 6), which is the second most prevalent forest class, covering 4.7% of the classified area (Table 4). The temperate deciduous forest class (cluster 9) was much less extensive (Table 4) and was confined to two distinct stands (Figure 6). The hummock class (cluster 2) covered 3.7% of the classified area (Table 4). Occurrences of this type were more scattered and varied in size considerably (Figure 6).

We mapped several other land cover types that exist on MCRDPI to provide a continuous land cover and vegetation map that is required for ongoing management and conservation decision-making. Here, we briefly describe the concepts of those land cover types. The developed forest type has an overstory of widely spaced trees (often *Quercus virginiana* or *Pinus elliottii*) with no mid-story or shrub layer, and an understory of non-native lawn grasses. Both the developed forest and mowed lawn types represent human-modified vegetation around areas of infrastructure that are maintained by mowing and collectively cover 10.2% of

Table 4. Total area covered by the 23 land cover types in the vegetation map. USNVC Associations are included for those types that were identified using cluster analysis of vegetation plot data.

Land Cover Type	Cluster	Associations	Area (m²)	Area (%)
Bare Ground	N/A	N/A	133895	0.38
Beach	N/A	N/A	169060	0.47
Brackish Marsh	4	CEGL008742	286895	0.81
Developed Forest	N/A	N/A	463645	1.30
Dune	N/A	N/A	295508	0.83
Hard Marsh	5	CEGL004191	1067360	3.00
Hummock	2	CEGL007813	1332680	3.74
Infrastructure	N/A	N/A	2418420	6.79
Maritime Forest	11, 12	CEGL007032, CEGL007027	1804900	5.07
Mixed Forest	10	CEGL007726	87245	0.25
Mowed Lawn	N/A	N/A	3158510	8.87
Open Pine Woodland	6	CEGL004864	1670960	4.69
Pine Forest w/ Maritime Influence	8	CEGL004658	1063620	2.99
Pine Regeneration	N/A	N/A	114781	0.32
Pine Woodland w/ Maritime Influence	7	CEGL004658	402959	1.13
Saline Shrubland	1	CEGL003924	348697	0.98
Salt Flat	3	CEGL002278	866915	2.44
Salt Scrub	N/A	N/A	16851	0.05
Soft Marsh	5	CEGL004191	14719126	41.35
Successional Shrubland	N/A	N/A	103124	0.29
Temperate Deciduous Forest	9	CEGL004747	52690	0.15
Water	N/A	N/A	4962560	13.94
Yaupon Forest	N/A	N/A	58184	0.16

the classified area (Table 4). Dune, which represents areas of sandy coastline covered by shell deposits, along with coastal grass and succulent species, is present along beaches that occur on the western edge of MCRDPI. Beach represents sandy, non-vegetated areas of the coastline immediately adjacent to dunes. Small occurrences of other vegetation types exist across the island, covering 1.3% of the classified area combined (Table 4). These types include successional shrubland, which is a ruderal, shrub dominated type that occurs as an early successional stage following clear cutting or burning. Pine regeneration is a similar successional type strongly dominated by regenerating pine seedlings and saplings. Yaupon forest is a type occurring primarily in areas with a history of significant anthropogenic disturbance and hence forest composition is highly variable depending on the pre-disturbance vegetation. However, *Ilex vomitoria* (yaupon holly) often occurs as thickets in this type.

The accuracy assessment performed for the map indicated an overall accuracy of 62.3% and a kappa statistic of 0.6. Several land cover types had producer's and user's accuracy over 0.7, indicating these types had higher overall accuracy. This included water, mowed lawn, infrastructure, temperate deciduous forest, and pine forest with maritime influence (Suppl. material 1). Collectively, these types represent 32.7% of MCRDPI. The most extensive vegetation type on MCRDPI (soft marsh, covering 41.4%) had a producer's and user's accuracy of 84% and 58%, respectively. For soft marsh, 26% of misclassified points were classified to hard marsh instead, a closely related type also characterized by a monospecific community of *Spartina alterniflora* but found at higher elevation with shorter plant height (Suppl. material 2). Hard marsh, which covered 3% of MCRDPI, had a user's accuracy of 75% and when misclassification occurred, points were assigned to closely related marsh types (i.e., soft marsh and salt flat) (Suppl. material 2). When soft marsh and hard marsh were combined into a single type, the resulting user's accuracy for the combined *Spartina alterniflora* type was 82.9%. Additional land cover types with moderate accuracy (both producer's and user's accuracy between 0.6 and 0.7) included: beach, hummock, and pine regeneration (Suppl. material 1). Several forest types (mixed forest, pine woodland with maritime influence, maritime forest, and yaupon forest) had relatively low accuracy (Suppl. material 1), which we attribute to poor separability between forest types due to similar spectral signatures, rather than random misclassification. However, many of these classes with low producer's or user's accuracy that decreased the overall accuracy were not very common (e.g., bare ground, mixed forest, yaupon forest, each comprising <0.25% of MCRDPI).

Discussion

Our primary objective was to characterize the vegetation types present on a sea island in South Carolina, USA, and to map their distribution. This region was recently identified as a global hotspot for salt marsh loss (Cazenave and Cozannet 2014; Rutledge et al. 2021; White et al. 2022) and the 2022 vegetation map we produced will serve as an anchor point for evaluating salt marsh decline and die-off in the recent past and under future conditions. We identified 12 distinct vegetation types from vegetation plot data and cross-walked them onto 11 existing USNVC Associations, many of which are common, widely distributed types within the southeastern USA. We mapped 11 additional land cover type classes, for a total of 23 unique land cover types. MCRDPI is primarily dominated by marsh habitats (covering 49% of the classified area), while forested types covered 20.1% collectively. Several environmental variables, most importantly salinity and elevation, were significantly related to the species composition patterns of the 12 vegetation types we documented.

As expected, marsh types generally had higher salinity and occurred at lower elevations than forest types. The dominant salt marsh type (cluster 5) occurred as monotypic stands of *Spartina alterniflora*, an extremely salt tolerant perennial grass that dominates the low marsh of many coastal wetlands throughout the eastern USA (Humphreys et al. 2021). As salinity decreased and elevation generally increased further inland, the salt marsh transitioned into high marsh types including salt flats (cluster 3) and saline shrublands (cluster 1). Hummocks (cluster 2) occurred as higher elevation islands with lower salinity within the surrounding marsh landscapes and supported more diverse assemblages. The brackish marsh type (cluster 4) occurred in low lying depressions along the edges of upland forests. The surrounding landscape enabled tidal flooding to still influence these areas, despite their inland location. These results are consistent with other studies that have documented salinity (Watson and Byrne 2009; Tiner 2013; Woods et al. 2020) and elevation (Costa et al. 2003) as significant drivers of coastal habitat zonation.

The primary environmental variables that influenced the distribution of the forest types on MCRDPI were elevation and distance from shoreline. The maritime forest types (clusters 11 and 12) primarily occurred closer to the coastline than other forest types. These types are characterized by canopies shaped by salt spray, species more tolerant of salinity, and well- drained soils (Sandifer et al. 1980). Cluster 12 had the highest percentage sand, facilitating drainage which may reduce the accumulation of salt in areas supporting this type. Further inland, pine dominated types (clusters 6–8) occurred at higher elevations and were protected from salt spray that influenced the maritime forest types (Sandifer et al. 1980). The stand of temperate deciduous forest (cluster 9) was in the center of the island at relatively high elevation. These deciduous hardwood assemblages are very sensitive to salinity and are typically found at higher elevations in coastal settings in locations that are isolated from salt spray and tidal influence (Anderson et al. 2022).

Management activities also influenced the distribution of forest types. Upland pine-dominated forests and woodlands in the North American Coastal Plain have evolved with fire and are considered fire-dependent ecosystems (Noss et al. 2015; Glitzenstein et al. 2021). Prescribed fire

that mimics historical fire regimes of the region (generally low severity fire every 2–5 years) has been implemented in the pine-dominated types on MCRDPI to maintain or open the canopy and promote herbaceous cover in the understory layer. The goal of prescribed fire management, which is sometimes coupled with mechanical thinning, is to enhance habitat for open-canopy specialists on MCRDPI, such as the eastern diamondback rattlesnake and southern fox squirrel. The extensive stand of open pine woodland (cluster 6) surrounding Page Field is the result of these management practices. In the absence of fire, these types can be invaded by hardwoods (Rutledge et al. 2021), such as *Quercus nigra* and *Liquidambar styraciflua*, and become more closed canopy, transitioning to mixed forests (cluster 10). A few other types were mapped as either successional types that formed after timber harvest (i.e., successional shrubland and pine regeneration) or as ruderal types that have established in areas with a history of other significant human disturbances (i.e., yaupon forest).

Overall, we were successful in mapping most of the fine scale vegetation types using high resolution RGB imagery over a relatively small area. The overall accuracy of our map was 62.3% with a kappa statistic of 0.6, which suggests moderate support for the map and is within the range of accuracies achieved in other salt marsh classification studies (59 to 99%) (Rosso et al. 2006; Sadro et al. 2007; Wang et al. 2007; Hladik et al. 2013). Traditionally, an overall accuracy target has consistently been 80%, suggesting high support. However, recently some have argued that this value may be an unrealistic goal for certain mapping applications, particularly those mapping vegetation at fine scales over a relatively small area (Foody 2008), as in our study. We did not explicitly identify an accuracy threshold and instead interpreted the accuracy of the vegetation distribution map in the context of each individual classes' accuracy values to identify areas of improvement. We achieved moderate to high accuracy for many land cover types which comprise a significant portion of MCRDPI, including the dominant vegetation type (soft marsh). This was especially true when soft marsh and hard marsh were combined into a single marsh type as both are dominated by *Spartina alterniflora* and are only separated by subtle differences in vegetation height and elevation. There were some types that had poor separability due to significant overlap of their spectral signatures, which was indicated by low producer's and user's accuracy. Mixed forest, pine woodland with maritime influence, and yaupon forest were all challenging to map because the canopy of these types shared a lot of species with other forest types. Other challenging types were those that were not very extensive on MCRDPI, including bare ground and salt scrub. This suggests that the map does not currently accurately represent these classes and some caution should be implemented when interpreting their distributions. Minor discrepancies between the 2022 mapped type and land cover type on the ground could have occurred because most field validation points were collected in summer 2024 (two and a half years after the imagery was collected) and changes in the habitat type could have occurred over that period of time. We know of at least once instance of this: in 2022 an area was mapped as mowed lawn within a campground, but the expansion of the campground and new roads resulted in the assignment of the validation point to infrastructure in 2024. Additionally, some misclassification could have occurred as we were unable to identify the tidal stage for the 2022 imagery. Ideally, imagery is collected during low tide conditions to avoid misclassifying salt marsh as water (Campbell et al. 2017). Thus, depending on the tidal stage of the 2022 imagery, some pixels may have been misclassified as water when they were really salt marsh. Additional training point collection on future imagery, as well as imagery with higher spectral resolution, especially infrared spectral bands, and high-resolution elevation data (e.g., LiDAR) could achieve better model performance (Simas et al. 2001; Lucas and Carter 2013; Bid 2016), likely improving the separability of these classes and thus the overall accuracy of the model. If separability cannot be improved, then it may be warranted to combine these class groupings into single classes. Overall, the accuracy assessment revealed moderate support for the 23 land cover types and high support for several widely distributed types (e.g., soft and hard marsh). As most management activities and habitat analyses will not require vegetation types mapped as finely as we have, the vegetation map in its current form is likely to be a useful tool on MCRDPI, especially for activities that require distinguishing forests, woodlands, and marsh.

For some vegetation types, our descriptions are based on a small number of plots because those types are uncommon on MCRDPI and because the spatial extent of our study area is relatively small. While many of the sites fit their descriptions well, there is considerable compositional variability within natural vegetation types that ideally warrants description of types based on large numbers of vegetation plots. At the same time, sampling vegetation plots in close proximity may not generate new information about a vegetation type. We chose to address these challenges by sampling fewer plots in vegetation types that were infrequent on MCRDPI. For example, there is one primary temperate deciduous forest patch on the island, where we sampled two plots. Sampling more plots in that patch is unlikely to yield new information about that type and is time intensive. Future sampling efforts will target the more heterogenous types that are perhaps under-represented by plot data to refine type descriptions. Despite those limitations, we were able to successfully align our vegetation types with existing USNVC Associations.

Surveying and documenting the existing vegetation types and their distributions on MCRDPI provides important baseline data that future work can build off. This initial data paired with future survey data will facilitate more accurate mapping and delineation of distribution changes. Long term monitoring of vital coastal ecosystems, particularly on sea islands and barrier islands, will provide further insight into the impact of SLR on these habitats. Paired with the vegetation surveys, classification of imagery will facilitate improvement of the deep learning model and can be used with the current map that we

presented here to conduct change detection analyses to identify changes in the distribution of vegetation types in the recent past or future and whether they can be attributed to SLR or increased storm surge activity. This map and the associated vegetation survey data is already being used on MCRDPI to quantify habitat use by wildlife species of conservation concern, carbon storage in different land cover types, and to understand how salt marsh migration might be impeded by infrastructure and the effects of land cover type on heat stress experienced during military training. Like other vegetation classification and mapping efforts, it has the potential to inform conservation efforts and decision-making within a region that is experiencing rapid change due to compounding global change factors.

Data availability

Data are available upon request.

Author contributions

CG and KP planned the research and conducted vegetation surveys, JH evaluated and sought approval for soil sampling at the vegetation plots and provided information about the ecology of Parris Island, CG conducted statistical analyses and image classification and led the writing, AA provided guidance on the image classification approach, PP provided guidance on the vegetation survey and classification methodology, ZB and KP conducted the accuracy assessment, and all authors edited the manuscript.

Acknowledgements

Funding was provided by the Department of Navy, Marshall University, and the NASA West Virginia Space Grant Consortium. We thank Evan Donnachie for help with field data collection associated with the accuracy assessment.

References

Alizad K, Hagen SC, Medeiros SC, Bilskie MV, Morris JT, Balthis L, Buckel CA (2018) Dynamic responses and implications to coastal wetlands and the surrounding regions under sea level rise. PLoS ONE 13: e0205176. https://doi.org/10.1371/journal.pone.0205176

Anderson SM, Ury EA, Taillie PJ, Ungberg EA, Moorman CE, Poulter B, Ardón M, Bernhardt ES, Wright JP (2022) Salinity thresholds for understory plants in coastal wetlands. Plant Ecology 223: 323–337. https://doi.org/10.1007/s11258-021-01209-2

Bertness MD, Gough L, Shumway SW (1992) Salt tolerances and the distribution of fugitive salt marsh plants. Ecology 73: 1842–1851. https://doi.org/10.2307/1940035

Bid S (2016) Change detection of vegetation cover by NDVI technique on catchment area of the Panchet Hill Dam, India. International Journal of Research in Geography 2: 11–20. https://doi.org/10.20431/2454-8685.0203002 [IJRG]

Cahoon DR, McKee KL, Morris JT (2021) How plants influence resilience of salt marsh and mangrove wetlands to sea-level rise. Estuaries and Coasts 44: 883–898. https://doi.org/10.1007/s12237-020-00834-w

Campbell JB (2006) Introduction to remote sensing. 4th ed. The Guilford Press, New York, NY.

Campbell A, Wang Y, Christiano M, Stevens S (2017) Salt marsh monitoring in Jamaica Bay, New York from 2003 to 2013: A decade of change from restoration to Hurricane Sandy. Remote Sensing 9: 131. https://doi.org/10.3390/rs9020131

Cazenave A, Cozannet GL (2014) Sea level rise and its coastal impacts. Earth's Future 2: 15–34. https://doi.org/10.1002/2013EF000188

Costa CSB, Marangoni JC, Azevedo AMG (2003) Plant zonation in irregularly flooded salt marshes: Relative importance of stress tolerance and biological interactions. Journal of Ecology 91: 951–965. https://doi.org/10.1046/j.1365-2745.2003.00821.x

Cunha-Lignon M, Kampel M, Menghini RP, Schaeffer-Novelli Y, Cintrón G, Dahdouh-Guebas F (2011) Mangrove forests submitted to depositional processes and salinity variation investigated using satellite images and vegetation structure surveys. Journal of Coastal Research SI 64: 344–348. https://www.jstor.org/stable/e26482118

Dave RN (1991) Characterization and detection of noise in clustering. Pattern Recognition Letters 12: 657–664. https://doi.org/10.1016/0167-8655(91)90002-4

De Cáceres M, Font X, Oliva F (2010) The management of vegetation classifications with fuzzy clustering. Journal of Vegetation Science 21: 1138–1151. https://doi.org/10.1111/j.1654-1103.2010.01211.x

Donnelly JP, Bryant SS, Butler J, Dowling J, Fan L, Hausmann N, Newby P, Shuman B, Stern J, Westover K, Webb T III (2001) 700 yr sedimentary record of intense hurricane landfalls in southern New England. GSA Bulletin 113: 714–727. https://doi.org/10.1130/0016-7606(2001)113%3C0714:YSROIH%3E2.0.CO;2

Du J, Hesp PH (2020) Salt spray distribution and its impact on vegetation zonation on coastal dunes: A review. Estuaries and Coasts 43: 1885–1907. https://doi.org/10.1007/s12237-020-00820-2

Faber-Langendoen D, Keeler-Wolf T, Meidinger D, Tart D, Hoagland B, Josse C, Navarro G, Ponomarenko S, Saucier JP, … Comer P (2014) EcoVeg: A new approach to vegetation description and classification. Ecological Monographs 84: 533–561. https://doi.org/10.1890/13-2334.1

Feagin RA, Smith WK, Psuty NP, Young DR, Martínez ML, Carter GA, Lucas KL, Gibeaut JC, Gemma JN, Koske RE (2010) Barrier islands: Coupling anthropogenic stability with ecological sustainability. Journal of Coastal Research 26: 987–992. https://doi.org/10.2112/09-1185.1

Field C, Gjerdrum C, Elphick C (2016) Forest resistance to sea-level rise prevents landward migration of tidal marsh. Biological Conservation 201: 363–369. https://doi.org/10.1016/j.biocon.2016.07.035

Foody GM (2008) Harshness in image classification accuracy assessment. International Journal of Remote Sensing 29: 3137–3158. https://doi.org/10.1080/01431160701442120

Franklin S, Faber-Langendoen D, Jennings M, Keeler-Wolf T, Loucks O, Peet R, Roberts D, McKerrow A (2012) Building the United States national vegetation classification. Annali di Botanica 2: 1–9.

Glitzenstein JS, Brewer JS, Masters RE, Varner JM, Hiers JK (2021) Chapter 3: fire ecology and management of southeastern Coastal Plain pine ecosystems. In: Greenberg CH, Collins B (Eds) Fire ecology and management: past, present, and future of US forested

ecosystems. Springer Nature, New York, NY, 63–104. https://doi.org/10.1007/978-3-030-73267-7_3

Gonzalez-Perez A, Abd-Elrahman A, Wilkinson B, Johnson DJ, Carthy RR (2022) Deep and machine learning image classification of coastal wetlands using unpiloted aircraft system multispectral images and lidar datasets. Remote Sensing 14: 3937. https://doi.org/10.3390/rs14163937

He Q, Silliman BR (2019) Climate change, human impacts, and coastal ecosystems in the Anthropocene. Current Biology: CB 29: R1021–R1035. https://doi.org/10.1016/j.cub.2019.08.042

Hladik C, Schalles J, Alber M (2013) Salt marsh elevation and habitat mapping using hyperspectral and LIDAR data. Remote Sensing of Environment 139: 318–330. https://doi.org/10.1016/j.rse.2013.08.003

Humphreys A, Gorsky AL, Bilkovic DM, Chambers RM (2021) Changes in plant communities of low-salinity tidal marshes in response to sea-level rise. Ecosphere 12: e03630. https://doi.org/10.1002/ecs2.3630

Jennings MD, Faber-Langendoen D, Loucks OL, Peet RK, Roberts D (2009) Standards for associations and alliances of the U.S. National Vegetation Classification. Ecological Monographs 79: 173–199. https://doi.org/10.1890/07-1804.1

Kearney WS, Fernandes A, Fagherazzi S (2019) Sea-level rise and storm surges structure coastal forests into persistence and regeneration niches. PLoS ONE 14: e0215977. https://doi.org/10.1371/journal.pone.0215977

Kirwan ML, Gedan KB (2019) Sea-level driven land conversion and the formation of ghost forests. Nature Climate Change 9: 450–457. https://doi.org/10.1038/s41558-019-0488-7

Kirwan ML, Kirwan JL, Copenheaver CA (2007) Dynamics of an estuarine forest and its response to rising sea level. Journal of Coastal Research 23: 457–463. https://doi.org/10.2112/04-0211.1

Legendre P, De Cáceres M (2013) Beta diversity as the variance of community data: Dissimilarity coefficients and partitioning. Ecology Letters 16: 951–963. https://doi.org/10.1111/ele.12141

Lucas KL, Carter GA (2013) Change in distribution and composition of vegetated habitats on Horn Island, Mississippi, northern Gulf of Mexico, in the initial five years following Hurricane Katrina. Coastal Geomorphology and restoration 44th Binghamton Geomorphology Symposium 199: 129–137. https://doi.org/10.1016/j.geomorph.2012.11.010

Ma L, Liu Y, Zhang X, Ye Y, Yin G, Johnson BA (2019) Deep learning in remote sensing applications: A meta-analysis and review. ISPRS Journal of Photogrammetry and Remote Sensing 152: 166–177. https://doi.org/10.1016/j.isprsjprs.2019.04.015

Maechler M, Rousseeuw P, Struyf A, Hubert M, Hornik K (2022) cluster: cluster analysis basics and extensions. R package version 2.1.4. https://cran.r-project.org/web/packages/cluster/index.html [accessed 7 Dec 2022]

Maggiori E, Tarabalka Y, Charpiat G, Alliez P (2017) Convolutional neural networks for large-scale remote-sensing image classification. IEEE Transactions on Geoscience and Remote Sensing 55: 645–657. https://doi.org/10.1109/TGRS.2016.2612821

Marcot BG, Woo I, Thorne KM, Freeman CM, Guntenspergen GR (2020) Habitat of the endangered salt marsh harvest mouse (*Reithrodontomys raviventris*) in San Francisco Bay. Ecology and Evolution 10: 662–677. https://doi.org/10.1002/ece3.5860

McCune B, Grace JB (2002) Analysis of ecological communities. MjM Software Design, Gleneden Beach, Oregon, US.

Murray NJ, Worthington TA, Bunting P, Duce S, Hagger V, Lovelock CE, Lucas R, Saunders MI, Sheaves M, … Lyons MB (2022) High-resolution mapping of losses and gains of Earth's tidal wetlands. Science 376: 744–749. https://doi.org/10.1126/science.abm9583

Naumann JC, Young DR, Anderson JE (2009) Spatial variations in salinity stress across a coastal landscape using vegetation indices derived from hyperspectral imagery. Plant Ecology 202: 285–297. https://doi.org/10.1007/s11258-008-9482-2

NOAA (2023) Climate at a glance county mapping. https://www.ncei.noaa.gov/access/monitoring/climate-at-a-glance/county/mapping/110/pcp/202201/12/value [accessed 13 October 2023]

Noss RF, Platt WJ, Sorrie BA, Weakley AS, Means DB, Costanza J, Peet RK (2015) How global biodiversity hotspots may go unrecognized: Lessons from the North American Coastal Plain. Diversity & Distributions 21: 236–244. https://doi.org/10.1111/ddi.12278

Oksanen J, Simpson GL, Blanchet FG, Kindt R, Legendre P, Minchin PR, O'Hara RB, Solymos P, Stevens HMH, … Weedon J (2022) vegan: community ecology package. R package version 2.3-2. http://cran.r-project.org/package=vegan [accessed 7 Dec 2022]

Olofsson P, Foody GM, Herold M, Stehman SV, Woodcock CE, Wulder MA (2014) Good practices for estimating area and assessing accuracy of land change. Remote Sensing of Environment 148: 42–57. https://doi.org/10.1016/j.rse.2014.02.015

Osisanwo F, Akinsola J, Awodele O, Hinmikaiye J, Olakanmi O, Akinjobi J (2017) Supervised machine learning algorithms: Classification and comparison. International Journal of Computer Trends and Technology 48: 128–138. https://doi.org/10.14445/22312803/IJCTT-V48P126

Peet RK, Wentworth TR, White PS (1998) A flexible, multipurpose method for recording vegetation composition and structure. Castanea 63: 262–274. https://doi.org/10.2307/4033979

Peet RK, Lee MT, Boyle MF, Wentworth TR, Schafale MP, Weakley AS (2012) Vegetation-plot database of the Carolina Vegetation Survey. Biodiversity & Ecology 4: 243–253. https://www.biodiversity-plants.de/biodivers_ecol/publishing/b-e.00081.pdf

R Core Team (2022) R: A language and environment for statistical computing. R Foundation for Statistical Computing, Vienna, AT.

RStudio Team (2024) RStudio: Integrated Development Environment for R. Posit Software, PBC.

Raposa KB, Weber RLJ, Ekberg MC, Ferguson W (2017) Vegetation dynamics in Rhode Island salt marshes during a period of accelerating sea level rise and extreme sea level events. Estuaries and Coasts 40: 640–650. https://doi.org/10.1007/s12237-015-0018-4

Reed DJ (1995) The response of coastal marshes to sea-level rise: Survival or submergence? Earth Surface Processes and Landforms 20: 39–48. https://doi.org/10.1002/esp.3290200105

Rosencranz JA, Thorne KM, Buffington KJ, Overton CT, Takekawa JY, Casazza ML, McBroom J, Wood JK, Nur N, … Ambrose RF (2019) Rising tides: Assessing habitat vulnerability for an endangered salt marsh-dependent species with sea-level rise. Wetlands 39: 1203–1218. https://doi.org/10.1007/s13157-018-1112-8

Rosso PH, Ustin SL, Hastings A (2006) Use of lidar to study changes associated with *Spartina* invasion in San Francisco Bay marshes. Remote Sensing of Environment 100: 295–306. https://doi.org/10.1016/j.rse.2005.10.012

Rousseeuw PJ (1987) Silhouettes: A graphical aid to the interpretation and validation of cluster analysis. Journal of Computational and Applied Mathematics 20: 53–65. https://doi.org/10.1016/0377-0427(87)90125-7

Rutledge BT, Cannon JB, McIntyre RK, Holland AM, Jack SB (2021) Tree, stand, and landscape factors contributing to hurricane damage in a coastal plain forest: Post-hurricane assessment in a longleaf pine landscape. Forest Ecology and Management 481: 118724. https://doi.org/10.1016/j.foreco.2020.118724

Sadro S, Gastil-Buhl M, Melack J (2007) Characterizing patterns of plant distribution in a southern California salt marsh using remotely sensed topographic and hyperspectral data and local tidal fluctuations. Remote Sensing of Environment 110: 226–239. https://doi.org/10.1016/j.rse.2007.02.024

Sandifer P, Calder D, Manzi J, Miglarese J, Barclay L (1980) Ecological characterization of the sea island coastal region of South Carolina and Georgia. Volume III. Biological Features. U.S. Fish and Wildlife Service, Office of Biological Sciences.

Schowengerdt RA (2007) Remote sensing, models, and methods for image processing. Academic Press, Burlington, MA, US.

Simas T, Nunes JP, Ferreira JG (2001) Effects of global climate change on coastal salt marshes. Ecological Modelling 139: 1–15. https://doi.org/10.1016/S0304-3800(01)00226-5

Soil Survey Staff (2019) Web soil survey. https://websoilsurvey.nrcs.usda.gov/app/ [accessed 12 November 2022]

Sousa AI, Lillebø AI, Pardal MA, Caçador I (2010) Productivity and nutrient cycling in salt marshes: Contribution to ecosystem health. Estuarine, Coastal and Shelf Science 87: 640–646. https://doi.org/10.1016/j.ecss.2010.03.007

Tiner R (2013) Tidal wetlands trimer: an introduction to their ecology, natural history, status, and conservation. University of Massachusetts Press, Amherst, MA. https://doi.org/10.2307/j.ctt5vk8qw

Tong XY, Xia GS, Lu Q, Shen H, Li S, You S, Zhang L (2020) Land-cover classification with high-resolution remote sensing images using transferable deep models. Remote Sensing of Environment 237: 111322. https://doi.org/10.1016/j.rse.2019.111322

USNVC (2025) United States National Vegetation Classification Database Version 3.0. Federal Geographic Data Committee, Vegetation Subcommittee. Washington D.C., US.

Vepraskas MJ, Richardson JL, Vepraskas MJ, Craft CB (2000) Wetland soils: genesis, hydrology, landscapes, and classification. CRC Press, Boca Raton, FL, US. https://doi.org/10.1201/9781420026238

Wang C, Menenti M, Stoll M-P, Belluco E, Marani M (2007) Mapping mixed vegetation communities in salt marshes using airborne spectral data. Remote Sensing of Environment 107: 559–570. https://doi.org/10.1016/j.rse.2006.10.007

Wang P, Fan E, Wang P (2021) Comparative analysis of image classification algorithms based on traditional machine learning and deep learning. Pattern Recognition Letters 141: 61–67. https://doi.org/10.1016/j.patrec.2020.07.042

Warren RS, Niering WA (1993) Vegetation change on a Northeast tidal marsh: Interaction of sea-level rise and marsh accretion. Ecology 74: 96–103. https://doi.org/10.2307/1939504

Watson EB, Byrne R (2009) Abundance and diversity of tidal marsh plants along the salinity gradient of the San Francisco Estuary: Implications for global change ecology. Plant Ecology 205: 113–128. https://doi.org/10.1007/s11258-009-9602-7

Weakley AS (2022) Flora of the southeastern United States. University of North Carolina Herbarium, North Carolina Botanical Garden, Chapel Hill, NC, US.

Webster PJ, Holland GJ, Curry JA, Chang HR (2005) Changes in tropical cyclone number, duration, and intensity in a warming environment. Science 309: 1844–1846. https://doi.org/10.1126/science.1116448

White EE, Ury EA, Bernhardt ES, Yang X (2022) Climate change driving widespread loss of coastal forested wetlands throughout the North American Coastal Plain. Ecosystems 25: 812–827. https://doi.org/10.1007/s10021-021-00686-w

Woods NN, Swall JL, Zinnert JC (2020) Soil salinity impacts future community composition of coastal forests. Wetlands 40: 1495–1503. https://doi.org/10.1007/s13157-020-01304-6

E-mail and ORCID

Cody Goodson (cgoodson27@gmail.com), ORCID: https://orcid.org/0009-0006-9541-7918
John Holloway (john.d.holloway@usmc.mil)
Zak H. Bartholomew (bartholome10@marshall.edu), ORCID: https://orcid.org/0009-0000-8520-3314
Anne C. Axel (axel@marshall.edu), ORCID: https://orcid.org/0000-0002-5297-972X
Pamela Puppo (pamela.puppo@marshall.edu), ORCID: https://orcid.org/0000-0002-5038-0238
Peyton Debowsky (peytondebowsky@gmail.com)
Kyle A. Palmquist (Corresponding author, palmquist@marshall.edu), ORCID: https://orcid.org/0000-0001-7665-4105

Supplementary material

Supplementary material 1
Producer's accuracy and user's accuracy for each of the 23 land cover types mapped on MCRDPI. (*.pdf).
Link: https://doi.org/10.3897/VCS.157787.suppl1

Supplementary material 2
Confusion matrix for the 23 land cover types mapped on MCRDPI. (*.pdf).
Link: https://doi.org/10.3897/VCS.157787.suppl2

Supplementary material 3
Dendrogram showing the final clustering solution of sites to one of the 12 clusters. (*.pdf).
Link: https://doi.org/10.3897/VCS.157787.suppl3